DRI #2475

74021

REPORT

Final Report

Contract No. 14-01-0001-1440

31 October 1968

AMPTIAC

A STUDY OF THE STRESS CORROSION SUSCEPTIBILITY OF CUPRO-NICKEL AND TITANIUM UNDER DESALINATION CONDITIONS

DISTRIBUTION STATEMENT A
Approved for Public Release
Distribution Unlimited

UNIVERSITY OF DENVER
DENVER RESEARCH INSTITUTE

Reproduced From
Best Available Copy

20000908 228

A STUDY OF THE STRESS CORROSION SUSCEPTIBILITY OF CUPRO-NICKEL AND TITANIUM UNDER DESALINATION CONDITIONS

Final Report

Contract No. 14-01-0001-1440

3 July 1967 - 3 October 1968

- Submitted to -

Office of Saline Water
U. S. Department of the Interior
Washington, D. C.

- Submitted by -

University of Denver
Denver Research Institute

31 October 1968

APPROVED FOR THE DIRECTOR BY:

William C. Hagel
Head, Metallurgy Division

PREPARED BY:

R. Norman Orava
Research Metallurgist

APPROVED BY:

Charles E. Lundin
Manager, Metal Studies

ABSTRACT

An investigation was conducted of the susceptibility to stress corrosion cracking of 90Cu-10Ni, 70Cu-30Ni, and two commercial grades of unalloyed titanium (TMCA 50A and 75A) for conditions characteristic of those encountered during desalination operations. Bent-beam specimens from sheet and tubing, and C-rings from tubing were exposed at or near the macroscopic yield stress to brackish well water, seawater, or sea-salt brines (7 and 11w/o total salt), at zero or 8.5 fps, at temperatures of 75, 204, or 250°F. These materials did not exhibit stress corrosion cracking under these conditions. In addition, titanium did not experience any detectable corrosive attack up to about 1000 hr. exposure. Within this period, however, the Cu-Ni alloys suffered severe impingement attack, yielding corrosion rates in the range 1 to 200 mpy, depending on the testing variables. It was concluded that titanium is, potentially, a far more reliable candidate material for desalination service than is cupro-nickel.

→ p 12

TABLE OF CONTENTS

		Page
	ABSTRACT	ii
	LIST OF TABLES	v
	LIST OF FIGURES	vi
1.	INTRODUCTION	1
2.	STRESS CORROSION BEHAVIOR	2
	2.1 Copper-Nickel Alloys	2
	2.2 Titanium	3
3.	MATERIALS AND PROPERTIES	4
	3.1 Selection of Materials	4
	3.2 Copper-Nickel	4
	3.3 Titanium	8
	3.4 Prestrained Material	10
4.	SALINE SOLUTIONS	12
5.	EXPERIMENTAL PROCEDURE	13
	5.1 Bend Fixtures	13
	5.2 Bent-Beam Stress Corrosion Specimens	15
	5.2.1 Dimensions	15
	5.2.2 Selection of Stress	15
	5.2.3 Role of Temperature in Stress Selection	16
	5.2.4 Determination of Strain	18
	5.2.5 Determination of Specimen Length	18
	5.3 C-Ring Specimens	19
	5.3.1 Dimensions	19
	5.3.2 Determination of Specimen Deflection	20
	5.4 Testing Temperatures	20
	5.5 Velocity Apparatus	21
	5.6 Metallographic Examination	25

TABLE OF CONTENTS (Cont.)

		Page
6.	EXPERIMENTAL RESULTS	27
	6.1 Stress Corrosion	27
	6.2 Corrosion	27
7.	DISCUSSION AND CONCLUSIONS	44
	7.1 Stress Corrosion	44
	7.2 Corrosion	45
8.	ACKNOWLEDGMENTS	48
9.	REFERENCES	49

LIST OF TABLES

Table No.		Page
1.	Suppliers' Chemical Analyses for Cu-Ni Alloys	5
2.	Mechanical Properties of Cu-Ni Alloys, as Given by Suppliers.	5
3.	Measured Room-Temperature Tensile Properties of Cu-Ni Alloys	7
4.	Average Grain Size of Cu-Ni and Titanium	7
5.	Suppliers' Chemical Analyses for Titanium	9
6.	Mechanical Properties of Titanium as Given by Suppliers.	9
7.	Measured Room-Temperature Tensile Properties of Titanium.	10
8.	Measured Room-Temperature Transverse Strength Properties in Tension of Cu-Ni Sheet Reduced 50% and Ti Sheet Reduced 40% by Cold Rolling	11
9.	Composition of Brackish Well Water from Roswell, New Mexico	12
10.	Measured Total Salt Content, Specific Gravity, and pH of Corrodents	12
11.	Typical Values of Applied Stress, Strain, and Length of Bent-Beam Stress Corrosion Sheet Specimens	17
12.	Conditions and Accumulated Times for Stress Corrosion Tests of Sheet Material at Room Temperature	28
13.	Conditions and Accumulated Times for Stress Corrosion Tests of Sheet Material at 204°F and 8.5 fps	29
14.	Conditions and Accumulated Times for Stress Corrosion Tests of Sheet Material at 250°F	30
15.	Conditions and Accumulated Testing Times for Stress Corrosion Tests of Tubing	31
16.	Corrosion Rates for Cu-Ni Alloys	33

LIST OF FIGURES

Figure No.		Page
1.	Bent-Beam Fixture, Specimen, and Mounting Device	14
2.	Coated Bend Fixtures Mounted on Teflon Impeller	22
3.	Condenser Lid Used to Cover Pyrex Test Vessels at 204°F	23
4.	GSC Baffle Plates	23
5.	Arrangement of Heating Elements and Test Vessels in Hot Air Chamber	24
6.	Pressure Vessels Used for Stress Corrosion Tests at 250°F	26
7.	Effect of Total Salt Content of Corrodent on the Average Corrosion Rate of Cu-Ni Sheet Tested at 8.5 fps	34
8.	Effect of Total Salt Content of Corrodent on the Pitting Rate of Cu-Ni Sheet Tested at 8.5 fps	35
9.	Effect of Exposure Temperature on the Average Corrosion Rate of Cu-Ni Sheet Tested at 8.5 fps	36
10.	Comparison of Average Corrosion and Pitting Rates of Cu-Ni Sheet Tested at 8.5 fps in 11% Sea-Salt Brine	37
11.	Surface Appearance of Typical 90Cu-10Ni Corrosion Coupons Exposed for 49 Days at 8 to 10 fps in 11% Sea-Salt Brine at Room Temperature	39
12.	Surface Appearance of 90Cu-10Ni and 70Cu-30Ni Stress Corrosion Specimens Exposed for 49 and 47 Days, Respectively, at 8.5 fps in 11% Sea-Salt Brine at Room Temperature	40
13.	Surface Appearance of 90Cu-10Ni Stress Corrosion Specimens Exposed for 49 Days at 8.5 fps in 11% Sea-Salt Brine at 204°F	41
14.	Surface Appearance of 70Cu-30Ni Stress Corrosion Specimens Exposed for 47 Days at 8.5 fps in 11% Sea-Salt Brine at 204°F	41

LIST OF FIGURES (Cont.)

Figure No.		Page
15.	Surface Appearance of 90Cu-10Ni Tube Specimens Exposed for 42 Days at 8.5 fps in 11% Sea-Salt Brine at 204°F. Top Left: Seamless C-ring; Top Right: C-ring With Weld Seam; Bottom: Longitudinal Bent-Beam	42
16.	Surface Appearance of 90Cu-10Ni Exposed for 43 Days in 11% Sea-Salt Brine at 250°F. Top: Sheet Cold-Rolled 50%; Center: Annealed Sheet; Bottom: Longitudinal Tube	42
17.	Surface Appearance of 70Cu-30Ni Exposed for 42 Days in 11% Sea-Salt Brine at 250°F. Top: Sheet Cold-Rolled 50%; Center: Longitudinal Tube; Bottom: Annealed Sheet	43
18.	Surface Appearance of 90Cu-10Ni (Top) and 70Cu-30Ni (Bottom) Exposed for 49 Days in 7% Sea-Salt Brine at Room Temperature	43

1. INTRODUCTION

In the selection of suitable candidate materials for seawater or brackish-water conversion installations, serious consideration must be given to their overall corrosion properties to ensure long-term structural stability. One aspect of corrosion behavior, which is often totally unpredictable, is failure of a specimen or component subjected to a tensile stress in a corrosive environment. A great deal is known about the stress corrosion cracking susceptibility of a given material in a specific environment. However, to the author's knowledge, no systematic investigations have been undertaken to study such behavior under the combined influence of elevated temperatures, dynamic conditions, and brine concentrations, which would be typical of those encountered in desalination operations.

This final report describes the results of a research program designed to yield this information for two copper-nickel alloys (90Cu-10Ni and 70Cu-30Ni) and unalloyed commercial titanium with two different purities (TMCA 50A and 75A). Concurrently, some corrosion data were generated, specifically for the Cu-Ni alloys.

2. STRESS CORROSION BEHAVIOR

2.1 Copper-Nickel Alloys

The only non-conference book[1] which is devoted exclusively to the observations and mechanisms of stress corrosion cracking in metals gives no indication that stress corrosion cracking is or ever has been a problem with Cu-Ni alloys exposed to seawater or sea-salt brine environments. No reference is made to any investigation concerning the subject, or to any service experience. Logan[1] states that the ammonium ion is considered to be the specific corrodent responsible for the cracking of copper-base alloys.

Uhlig, in his most recent text on corrosion[2], does not mention stress corrosion cracking in connection with saline solutions. Without citing the specific corrodent (it was a moist ammoniacal atmosphere) Uhlig reports some work of Thompson and Tracy[3] who found that 70Cu-30Ni is relatively resistant to stress corrosion cracking compared to copper alloys with 10 or 20% Ni.

Other recent reviews (e.g. Ref. 4, 5) also fail to mention any incidence of the occurrence of stress corrosion cracking in Cu-Ni alloys exposed to seawater and its concentrated brines. When stress corrosion cracking is discussed without specific mention of corrodent, the damaging species is the ammonium ion.

Let us consider the problem from another aspect. A survey of materials behavior in multi-stage flash distillation plants was conducted very recently by Arthur D. Little, Inc. The results, as yet unpublished except in the form of a brief summary report[6], were presented at a symposium in Washington sponsored by the Office of Saline Water. On that occasion, the authors revealed that there was no history of a stress corrosion failure of tubing or tube sheets in those MSFD plants. The materials used were arsenical aluminum brass, 90Cu-10Ni, 70Cu-30Ni, and titanium.

A slightly earlier review by Tuthill & Sudrabin[7] of the causes of failure in copper-base condenser tubes and condensers stated that 90Cu-10Ni and 70Cu-30Ni (both iron modified) are resistant to stress corrosion cracking in saline waters.

In summary, then, it would appear that there is nothing to indicate that Cu-Ni alloys are susceptible to stress corrosion cracking in saline environments. However, there is sufficient doubt about their performance at the extremes of the conditions encountered to warrant confirmation of this behavior.

2.2 Titanium

It is only since 1955 that attention was first focussed on the possibility of the stress corrosion failure of titanium alloys at elevated temperatures in the presence of hot salts. This recognition was further enhanced by Brown[8-10] in 1964 who showed that the combination of stress, salt water, time, and a preexisting crack can lead to the premature failure of many titanium alloys even at room temperature. Indeed, unalloyed commercial titanium, A-70[10] or RS-70[11] (equivalent to TMCA 75A), exhibits some decrease in toughness under these conditions. Yet, Ti-65A appears to be immune[12], presumably as a result of a slightly lower oxygen content. For some alloys, distilled water itself can have a detrimental effect[10,11].

There is a subtle difference between environmental embrittlement, or reduction in toughness, when a specimen is subjected to a room-temperature saline environment, and failure due to the presence of hot salt at elevated temperatures (>500°F). The latter represents stress corrosion cracking in the classical sense, whereas the former was, and still is, believed to require a severe preexisting stress-raiser[8-12]. Recently, Scully and his coworkers[13] have shown that the problem is far more serious; stress corrosion cracking of Ti-5Al-2.5Sn in 3% NaCl solutions at room temperature was obtained in the absence of fine surface notches or fatigue cracks.

That the combined presence of a stress and a saline environment can lead to cracking of specific alloys at room temperature does not imply, of course, the susceptibility of unalloyed titanium without a prior flaw. Rather, all indications[8,9], including limited service experience[6], are that a flaw must be a prerequisite. However, a wide gap exists between the ambient temperature seawater (or NaCl) and hot-salt conditions, wherein one finds the situation which is peculiar to desalination operations. There are no readily available data on stress corrosion resistance in flowing elevated-temperature solutions with larger salt contents (to 11%), and possibly pollutants as well. Therefore, as in the case of Cu-Ni, it would seem expedient to provide the designer with the required information.

3. MATERIALS AND PROPERTIES

3.1 Selection of Materials

Two copper-nickel alloys and two commercial grades of unalloyed titanium were selected for study. The Cu-Ni alloys originally proposed were pure 70Cu-30Ni, and 70Cu-30Ni with about 0.5 w/o Fe. However, the former could only be considered of academic interest since it is no longer commercially available and its corrosion properties are inferior to those of its iron-containing counterpart. Consequently, the pure 70Cu-30Ni was replaced by 90Cu-10Ni which, in turn, has about 1.25 w/o Fe. This alloy is appreciably less expensive than the 70Cu-30Ni, with corrosion properties only marginally less attractive. Accordingly, it is the more popular in current desalination service.

The choice of unalloyed titanium was based on its extremely good corrosion resistance in saline solutions. There was some doubt, however, concerning the purity necessary to preclude stress corrosion cracking. Therefore, two grades were investigated: TMCA designations Ti-50A and Ti-75A.

3.2 Copper-Nickel

The following sheet materials were supplied by Anaconda American Brass Company:

a. 90Cu-10Ni: 8 × 16 × 0.050 in.; annealed

b. 70Cu-30Ni: 8 × 16 × 0.050 in.; annealed

The tube materials received were:

a. 90Cu-10Ni: 1.00 in. O.D. × 0.063 in. wall × 12 ft.; welded (Valley Metal Works, California)

b. 70Cu-30Ni: 1.00 in. O.D. × 0.049 in. wall × 12 ft.; seamless (Scovill Mfg. Co.)

Except for the 90Cu-10Ni tubing, the chemical analyses and mechanical properties, as given by the suppliers, are listed in Tables 1 and 2, respectively. Valley Metal Works did not provide an analysis or any property data for their tubing. It is reasonable to assume that its chemical composition does not differ sufficiently from that of the sheet material to warrant an independent analysis.

In view of the method of load application, the yielding characteristics had to be known fairly accurately. Tensile tests on annealed sheet were conducted at room temperature and a strain rate of 3×10^{-4} sec^{-1} utilizing a Marquardt TM6 Universal Testing Machine. In almost all cases, strains were measured by means of an extensometer (LVDT) with a sensitivity of 5×10^{-5} in./in. Sheet specimens had gage dimensions of $1.0 \times 3/16 \times 0.050$ in. with the tensile axis oriented transverse to the original rolling direction. The tube materials were tested in an Instron Testing Machine, at a rate of 2×10^{-4} sec^{-1}. Specimens had gage dimensions of $2.0 \times 3/8 \times 0.03$ in.

TABLE 1. Suppliers' Chemical Analyses for Cu-Ni Alloys

	90Cu-10Ni	70Cu-30Ni	
Element	Sheet	Sheet	Tubing
Cu	87.96 w/o	68.86 w/o	68.7 w/o
Zn	<0.10	0.25	0.19
Pb	<0.02	0.005	<0.02
Fe	1.24	0.52	0.47
Ni	10.46	30.12	30.0
P	0.002	0.003	---
C	0.009	0.017	---
Mn	0.33	0.40	0.54

TABLE 2. Mechanical Properties of Cu-Ni Alloys, as Given by Suppliers

	90Cu-10Ni	70Cu-30Ni	
Property	Sheet	Sheet	Tubing
Young's Modulus (psi)	18×10^6	22×10^6	22×10^6
Yield Strength (psi; 0.5% offset)	22,000	22,000	26,000
Ultimate Strength	44,000	55,000	61,000
Rockwell Hardness	B33	B38	---

The tensile results are given in Table 3 for Cu-Ni. The data for sheet include as-machined material and that stress-relieved at 475°F for 1 hour*. A comparison of the strength values in Tables 2 and 3 reveals that the 90Cu-10Ni sheet is stronger than indicated by the manufacturer, and 70Cu-30Ni is weaker. This merely emphasizes the inadvisability of utilizing suppliers' data for performing the type of stress calculations which are required, for example, in this investigation.

The reason why the yield stress of 90Cu-10Ni is nearly 50% higher than that of 70Cu-30Ni is not clear. Taking into consideration that nickel does not appreciably harden copper, and assuming that both alloys have the same properties in the annealed state depending only on grain size (i.e. treating them as the same material), an estimate can be made of the grain-size sensitivity required to give the observed difference. As indicated in Table 4, the grain size of 90Cu-10Ni, as determined by the linear-intercept technique, is smaller than that of 70Cu-30Ni. If one now assumes further that this hypothetical material obeys the Hall-Petch relationship[14,15] between flow stress, σ_f, and grain diameter, ℓ,

$$\sigma_f = \sigma_0 + k\ell^{-1/2} \qquad (1)$$

then k is calculated to be 2.2 kg $mm^{-3/2}$ at 0.5% strain. This is twice the value of k for 70Cu-30Zn, which exhibits one of the highest grain-size sensitivities observed for face-centered cubic solid solutions[16]. On the basis of the quantity k/G, where G is the shear modulus, the grain-size dependence for Cu-Ni at 0.5% strain (0.39×10^{-3} $mm^{1/2}$) is within the range observed for molybdenum at the lower yield point ($0.30 - 0.42 \times 10^{-3} mm^{1/2}$). Molybdenum has one of the highest k-values (4-6 kg $mm^{-3/2}$)[16,17]. Adding this observation to the fact that the ultimate stress of 70Cu-30Ni is the larger, it is unlikely that a variation in grain size can account for the higher yield strength of 90Cu-10Ni relative to 70Cu-30Ni. Rather, the reversal in the sign of the strength difference in going from yield to ultimate strongly supports a contention that the strength difference at small strains is due to a higher dislocation density and more complex dislocation substructure in 90Cu-10Ni because of incomplete recrystallization. Iron precipitates may well have played a significant role in the inhibition of subgrain growth. The resolution of this question, by electron transmission studies, would have been very important had differences also been observed in stress corrosion behavior. Since they were not, the work was not considered pertinent to the program. This problem is not treated further in this report.

* ASM Metals Handbook, 8th Edition, Vol. 2, p. 285.

TABLE 3. Measured Room-Temperature Tensile Properties of Cu-Ni Alloys

	90Cu-10Ni			70Cu-30Ni		
	Sheet			Sheet		
Stress (psi)	A.M. (a)	S.R. (b)	Tubing	A.M.	S.R.	Tubing
Proportional Limit	22,000	17,000	26,700	13,000	11,000	19,600
Yield (0.2% offset strain)	28,100	27,000	37,200	18,300	17,200	32,300
Yield (0.5% total strain)	28,800	27,800	39,200	19,800	18,600	33,400
Yield (0.5% offset strain)	29,300	28,000	40,800	19,900	18,800	34,300
Ultimate	46,900	48,600	42,900	55,300	51,400	60,400

(a) as-machined
(b) stress-relieved

TABLE 4. Average Grain Size of Cu-Ni and Ti

Material	Form	Measured grain diameter (mm)	As given by Supplier (mm)
90Cu-10Ni	sheet	0.017	0.030
	tubing	0.050	(a)
70Cu-30Ni	sheet	0.045	0.060
	tubing	0.014	0.015
Ti-50A	sheet	0.016	(a)
	tubing	0.028	(a)
Ti-75A	sheet	0.015	(a)
	tubing	0.020	0.014

(a) not given

The magnitudes of the proportional limit indicate that the region over which stress can be considered directly proportional to strain, as related by Young's modulus, does not extend beyond a strain of about 0.1%. For stress-relieved 70Cu-30Ni, this may be as low as 0.04%, within the sensitivity of the present strain measurements. The strain estimates, discussed in Section 5.2 take this behavior into account.

It was evident from an examination of the microstructures that the grain morphology of both the annealed sheet and tubing is not a very sensitive function of orientation relative to the original rolling direction. Crystallographic textures were not evaluated since any cracking was expected to be intercrystalline.

Metallographic samples of Cu-Ni were prepared by polishing (10 volts, 30-45 sec.) and etching (5 volts, 15 sec.) electrolytically in a solution of 50% HNO_3 - 50% distilled water.

3.3 Titanium

The two grades of titanium to be investigated were originally specified as A-40 and A-70 which are Crucible Steel designations. Since equivalent material was obtained directly or indirectly from Titanium Metals Corporation of America, the appropriate respective designations of 50A and 75A are used here. The corresponding ASTM specifications for 50A and 75A sheet are B265-58, Grades 2 and 4, respectively, and for tubing, B338-65, Grades 2 and 4, respectively, where the lower grade number represents the purer form.

The following materials were received:

a. 50A sheet: 36 × 96 × 0.050 in., annealed (TMCA)

b. 50A tubing: 1.00 in. O.D. × 0.049 in. wall × 12 ft., seamless (TMCA)

c. 75A sheet: 8 × 36 × 0.050 in., annealed (TMCA)

d. 75A tubing: 1.00 in. O.D. × 0.040 in. wall × 12 ft., welded (Valley Metal Works, California).

The chemical analyses and mechanical properties as quoted by the suppliers are given in Tables 5 and 6, respectively. Grain sizes are shown in Table 4. To permit greater accuracy in the application of specified stresses, the strength properties were measured and are presented in Table 7. The yield strengths differ somewhat from quoted

TABLE 5. Suppliers' Chemical Analyses for Titanium

	50A		75A	
Element	Sheet	Tubing	Sheet	Tubing
C	0.023	0.027	0.023	0.025
Fe	0.06	0.09	0.18	0.13
N	0.014	0.018	0.015	0.011
H	0.003	0.002	0.002	0.003
O*	0.25(a)	0.25(b)	0.45(a)	0.40(b)

* Maximum oxygen content according to ASTM specification (a) B265-58T, and (b) B338-65, for Grades 2 and 4.

TABLE 6. Mechanical Properties of Titanium, as Given by Suppliers

	50A		75A	
	Sheet	Tubing	Sheet	Tubing
Young's modulus (10^6 psi)	14.9	14.9	15.1	15.1
Yield Strength (psi) - 0.2% offset	48,500	40,200	75,500	73,600
Ultimate	65,000	60,100	102,000	81,500

typical values (Table 6) but are within the max. - min. limits given. More important, the stress-strain curves revealed that all subsequent determinations of stress from applied strain for Ti sheet, but not tubing, could be made using the modulus to stresses just short of the upper yield point.

TABLE 7. Measured Room-Temperature Tensile Properties of Titanium

	50A		75A	
Stress (psi)	Sheet	Tubing	Sheet	Tubing
Proportional Limit	49,200	37,000	80,200	45,300
Upper Yield	49,800	---	84,900	---
Lower Yield	46,600	---	81,500	---
Yield (0.2% offset)	---	48,800	---	64,700
Ultimate	57,700	66,500	94,000	78,200

An examination of the microstructures of the as-received annealed sheet and tubing did not reveal any differences in grain morphology in the rolling plane, longitudinal, and transverse sections. The final metallographic preparation entailed the use of a combined polishing and etching operation on a Microcloth saturated with 0.05 micron alumina and Kroll's reagent (2 cc HF, 3 cc HNO_3, 95 cc distilled water), followed by a rinse and a further swab with Kroll's etchant for about 10 sec.

3.4 Prestrained Material

In order to assess the effect of plastic deformation (or hardness temper) on stress corrosion cracking susceptibility, the sheet materials were cold rolled to the following reductions without intermediate annealing:

Cu-Ni - 11, 21, and 50%

Ti - 11, 21, and 40%

The intention was to test the 40 and 50% reduced material first and then that with a lower prestrain if cracking was observed. The transverse strength properties are detailed in Table 8.

TABLE 8. Measured Room-Temperature Transverse Strength Properties in Tension of Cu-Ni Sheet Reduced 50% and Ti Sheet Reduced 40% by Cold-Rolling

Stress (psi)	90Cu-10Ni	70Cu-30Ni	Ti-50A	Ti-75A
Proportional limit	40,600	60,400	52,400	79,700
Yield (0.2% offset)	66,000	79,700	88,000	114,600
Ultimate	69,700	83,800	92,600	125,800

4. SALINE SOLUTIONS

The corrodents used in this investigation included brackish well water (feedwater to the OSW Demonstration Plant in Roswell, N.M.), San Diego Bay water (feedwater to the OSW San Diego Saline Test Facility), and sea-salt brine out of the San Diego facility. This latter is termed simply 7% brine. A recent Roswell analysis of the untreated brackish water is given in Table 9. The total salt content, specific gravity, and pH of the solutions are listed in Table 10. In addition, a more concentrated sea-salt brine solution was prepared from the 7% brine by adding to it sufficient salt obtained by evaporation of the 7% brine to bring the total salt content to 11%. Thus, the 11% brine contains the same solids that might normally be present if the solution were to have come directly from a conversion installation.

TABLE 9. Composition of Brackish Well Water From Roswell, New Mexico

Total Dissolved Solids	14,977 ppm
Sodium	4,925
Magnesium	165
Calcium	521
Iron	4.8
Chloride	7,860
Bicarbonate, etc.	156
pH	7.107
Specific Gravity	1.0080 at 34°C

TABLE 10. Measured Total Salt Content, Specific Gravity, and pH of Corrodents

Solution	Total Salt Content (w/o)	Specific Gravity (at 25°C)	pH
Brackish water	1.50	1.010	7.1
San Diego Bay water	3.92	1.027	8.0
San Diego brine - 7%	6.79	1.046	7.2
Prepared brine - 11%	10.72	1.071	9.2

5. EXPERIMENTAL PROCEDURE

5.1 Bend Fixtures

The first set of snap-in bend fixtures, 6 in. long and 0.75 in. wide, were machined from 3/16 in. 2024-T3 aluminum alloy plate. To prevent galvanic coupling between fixture and specimen, the fixtures were coated completely with a heat-resistant elastomer (RTV-11; G.E.). It soon became clear, however, that this combination of aluminum alloy and coating did not perform satisfactorily under certain conditions. The RTV stood up extremely well in brackish water at 75°F and 204°F under dynamic conditions but deteriorated in 11% brine at ambient temperature even in a static test. The deleterious effects were enhanced somewhat at 8.5 fps. Whatever the cause of the breakdown of the RTV in brine, and it did not appear to be an erosion effect, the result was a severe localized corrosion of the fixture. This is understandable, of course, since Al-Cu alloys are relatively active and highly susceptible to intergranular corrosion in chloride solutions. Rather than change the general type of coating, which does have favorable erosion, thermal, and adhesive qualities, bend fixtures were made from 1/8 in. Ti-75A sheet. Although titanium is less economical than 2024-T3 the weight advantage was maintained. Moreover, milling costs were eliminated by attaching the end load-bearing pieces to the main span with stainless steel rivets. Thus, when testing titanium, coating was restricted to the rivet heads. It was also found that a Dow Corning counterpart of the G.E. RTV-11, i.e. Silastic A RTV, performed marginally better at elevated temperatures. Also, a "fast cure" catalyst (RTV Catalyst No. 2) is available from Dow Corning which permits curing in 20 min. instead of the 24 hours needed with RTV-11. With Silastic A and Ti fixtures no additional problems were encountered with coating breakdown.

When testing the heavily cold-rolled materials it was necessary to provide bend fixtures with a smaller span of about 4 in. This was dictated by the large specimen deflection required to obtain the specified outer fiber stress.

Figure 1 shows a fixture, specimen, and the mounting device designed to facilitate insertion of the sample in the fixture.

The corrected jig span, H, was calculated from measurements made after coating with silicone primer (SS-4004; G.E.) by taking into account a 12° undercut, specimen thickness, measuring-pin diameters,

P.15 →

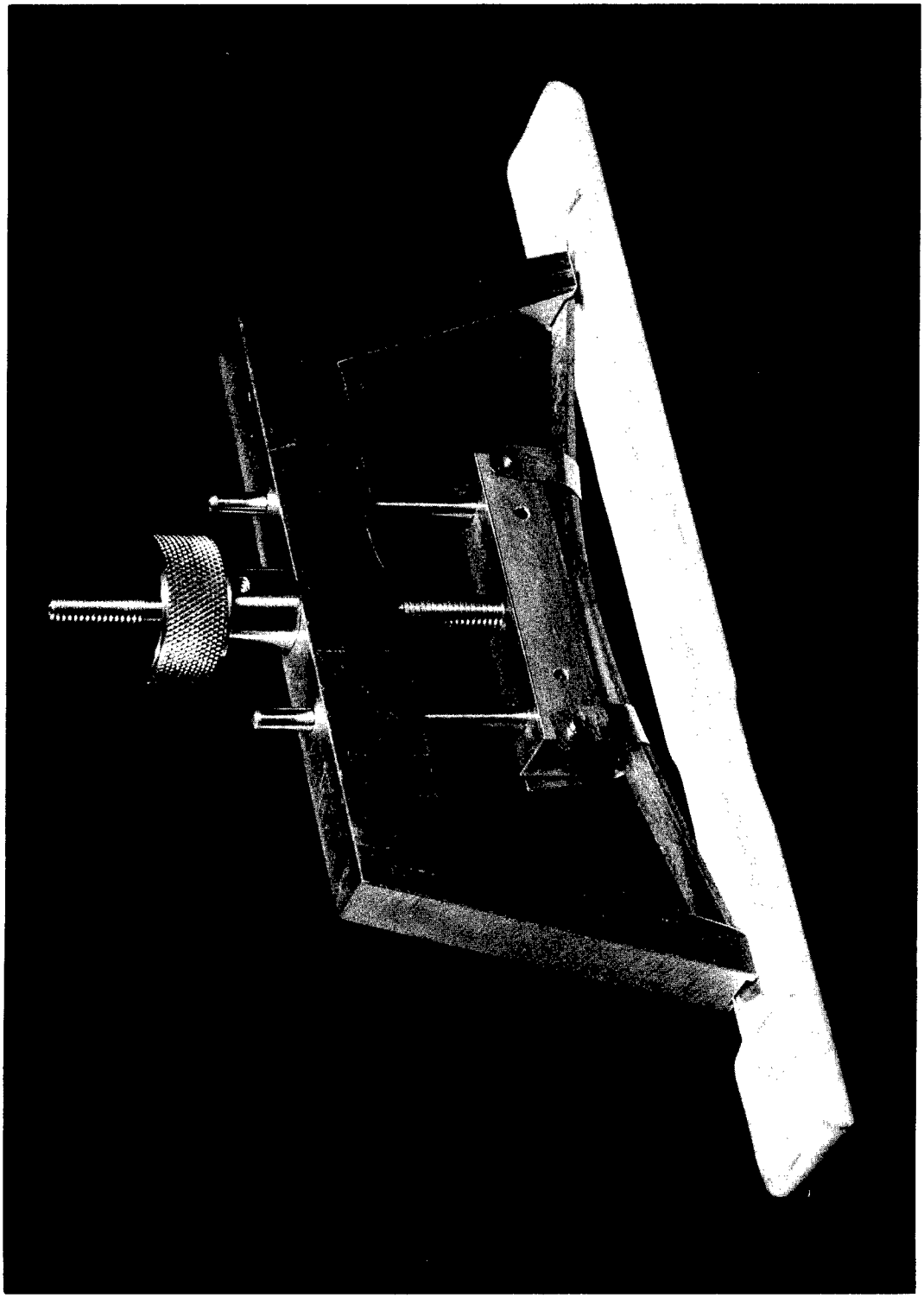

Figure 1. Bent-Beam Fixture, Specimen, and Mounting Device

and their location due to the undercut. The value of H is 4.9558 ± 0.0002 in. for the 2024-T3 jigs and 4.9553 ± 0.001 in. for the 75A. This difference does not contribute significantly to the specimen length calculation and consequently can be ignored.

5.2 Bent-Beam Specimens

5.2.1 Dimensions

The dimensions of the sheet bend specimens were 0.25 × 0.050 × L in., where L is the length, transverse to the original rolling direction. This represents the less susceptible of two possible "long transverse" orientations, but the difference in behavior would not be expected to be appreciable. "Longitudinal" samples of dimensions 0.25 × wall thickness × L in. were taken from tubing. Some included the weld seam. Similarly, prestrained samples were 0.25 × 0.025-0.030 × L in.

The majority of the stress-corrosion specimens were tested in the as-machined condition. A few of the initial exposures of Cu-Ni were performed with material which was stress relieved at 475°F for 1 hr. after machining. However, it was felt that the as-machined condition was the more likely to lead to cracking. Accordingly, stress-relieving was abandoned.

In no instance was the large surface of the specimens, corresponding to the original surface of the sheet, mechanically disturbed. It could be classified as good.

5.2.2 Selection of Stress

The establishment of stress-failure time relationships calls for the conduct of stress corrosion tests at various levels of stress approaching the macroscopic yield stress, σ_y. These increments are often, and likewise here, expressed as fractions of the yield stress. Also, it is logical to initiate the program at the highest stress level and then reduce this according to the outcome of the preceding experiments. This procedure was followed, where σ_y and applied stresses are specified more precisely below.

For annealed Ti sheet it was pointed out that Hooke's Law could be utilized over the whole stress range of interest. Room-temperature values of σ_y for 50A and 75A were taken as 48,000 psi and 83,000 psi, respectively, which are just less than the lowest observed upper yield

strengths. Thereupon, using an upper limit of about 0.9 σ_y insures that the applied stress is below the observed proportional limit and lower yield stress at ambient temperature.

For annealed and cold rolled Cu-Ni sheet, cold-rolled Ti sheet, and tubing of both materials, a significant departure from elastic behavior occurs at much smaller fractions of σ_y than for annealed Ti sheet. The value of σ_y for annealed Cu-Ni sheet and tubing was taken at 0.5% total strain and for Ti tubing, and cold-rolled Cu-Ni and Ti sheet, at 0.2% offset strain. The magnitudes of σ_y are summarized in the first column of Table 11.

Tests were commenced at a stress level of 0.99 for Cu-Ni, and 0.91 for Ti, followed by 0.90 and 0.75, respectively. Some typical values of applied stress and strain for sheet materials are given in Table 11.

5.2.3 Role of Temperature in Stress Selection

It is important to establish at the outset the reference temperature being used for σ_y when elevated temperature stress corrosion tests are conducted. Clearly, due to the strong temperature dependence of the yield stress of Ti[18] the application of a strain equivalent to 0.9 σ_y at room temperature results in appreciable plasticity at elevated temperatures. Therefore, the stress level is quoted as a fraction of both the room-temperature yield stress, σ_y, and the elevated-temperature value, $\sigma_y(T)$. High fractions of σ_y were used for all temperatures including 250°F. There is a very sound reason for doing this. Since structures are assembled at ambient temperatures, they may be subjected inadvertently to high elastic stresses which are sufficient to produce plastic flow during operation at elevated temperatures. Accordingly, some assesment of the effect of this plasticity on stress corrosion behavior is necessary. Constant-deflection type tests have the obvious advantage of permitting the application of high percentages of the room-temperature yield stress without mechanical failure of the specimens at higher temperatures.

The temperature dependence of the flow stress of the materials being studied is well established and is not subject to the same scatter as the absolute strength properties. Thus, once the yield stress is known for one temperature, relatively accurate estimates for other temperatures can be made from known sensitivities.

TABLE 11. Typical Values of Applied Stress, Strain, and Length of Bent-Beam Stress Corrosion Sheet Specimens

	Yield Stress, σ_y (psi)	Fraction of σ_y	Applied Stress (psi)	Total Strain (%)	Length of Specimen L(in.)
90Cu-10Ni (as-machined)	28,800	0.99	28,400	0.396	5.0402
90Cu-10Ni (stress-relieved)	27,800	0.99	27,400	0.396	5.0402
		0.90	25,100	0.210	4.9791
90Cu-10Ni (cold-rolled 50%)	66,000	1.00	66,000	0.567	4.4682
70Cu-30Ni (as-machined)	19,800	0.97	19,100	0.396	5.0402
70Cu-30Ni (stress-relieved)	18,600	0.97	18,000	0.396	5.0402
		0.90	16,700	0.230	4.9840
70Cu-30Ni (cold-rolled 50%)	79,700	1.00	79,700	0.562	4.4260
Ti-50A	48,000	0.91	43,500	0.291	5.0000
		0.75	36,100	0.242	4.9869
Ti-50A (cold-rolled 40%)	88,000	1.00	88,000	0.790	4.7852
Ti-75A	83,000	0.91	75,200	0.494	5.0858
		0.76	62,800	0.413	5.0459
Ti-75A (cold-rolled 40%)	114,600	1.00	114,600	0.960	5.2300

For Cu-Ni, the ratio of σ to σ_y can be considered to be independent of temperature for two reasons. Firstly, the flow stress is fairly insensitive to a change in temperature over the range of interest[19-21]. Secondly, even with some temperature sensitivity, the flow curves at different temperatures are roughly parallel in the strain range under consideration.

For Ti sheet, on the other hand, the preset strains are in the elastic range at room temperature but at elevated temperatures are in the plastic range due to the decrease in the yield stress. For example, $\sigma_y(204)$ is 76% of σ_y for 50A and 75A on the basis of 0.2% offset[22]. More comprehensive data[6] show that the proportional limit and lower yield stress of 75A at 204°F are 75.1% and 75.8%, respectively, of the room-temperature values. As a result, σ/σ_y and $\sigma(T)/\sigma_y(T)$ can be significantly different for Ti. The specific magnitudes of $\sigma(T)/\sigma_y(T)$ are presented with the elevated temperature data in the tables of Section 6.

5.2.4 Determination of Strain

Using the modulus line (Table 6) for annealed Ti sheet, examples of strains corresponding to 0.9 and 0.75 σ_y are given in Table 11.

The strains for Cu-Ni were determined from the plastic portion of the stress-strain curves, and typical values are shown in Table 11 for 0.99, 0.97, and 0.90 σ_y. The same procedure was followed with cold-rolled Ti sheet, and tubing of both materials.

5.2.5 Determination of Specimen Length

In order to achieve the desired outer fiber stress, equations developed by Haaijer and Loginow[23] for bent-beam stress corrosion specimens were utilized to calculate the specimen length, L. These are:

$$\epsilon = \frac{\sigma}{E} = \frac{2t}{H}\left[2E(k) - K(k)\right]\left[k - \frac{2E(k)-K(k)}{6}\right] \qquad (2)$$

and

$$\frac{L-H}{H} = \frac{2[K(k)-E(k)]}{2E(k)-K(k)} \qquad (3)$$

where

ϵ = tensile strain at the outer fiber

σ = tensile stress at the outer fiber

E = Young's modulus

t = specimen thickness

L = specimen length

H = jig span

K(k) = complete elliptical integral of the first kind

E(k) = complete elliptical integral of the second kind

Since these are parametric equations, a plot of ϵ against $\frac{L-H}{H}$ provides a graphical method for determining L. Although the point was already discussed above, the strain ϵ cannot be equated to σ/E unless Hooke's Law is obeyed, which is true only for annealed Ti sheet in this investigation. For this reason, Ketcham's expression[24] is not suitable. It should be noted that the latter equation is quoted incorrectly by Haynie and Boyd[25].

Using $t = 0.0500 \pm 0.0003$ in. for Cu-Ni and $t = 0.0510 \pm 0.0003$ in. for Ti, typical calculated specimen lengths are listed in Table 11.

In order to verify the validity of the specimen length determination, an SR-4 electrical-resistance strain gage was mounted on a 90Cu-10Ni specimen prior to its insertion in a bend fixture. The strain was calculated to be 0.00400 in./in. from the dimensions of the particular fixture and specimen ($0.99\sigma_y$) used. The measured strain was 0.00406 in./in., a difference of 1.5%. In view of the number of variables involved, this agreement must be considered excellent. Haaijer and Loginow[23] similarly established the suitability of their method. It is noteworthy that the residual strain was 0.00217 after removal from the fixture, thus confirming that $0.99\sigma_y$ is into the plastic range for Cu-Ni sheet.

5.3 C-Ring Specimens

5.3.1 Dimensions

The dimensions of the C-rings were 0.75 in. in the axial direction, with 1.0 in. outside diameter, and wall thicknesses of 0.0710 in., 0.0505 in., 0.0520 in., and 0.0420 in., for 90Cu-10Ni, 70Cu-30Ni, Ti-50A, and Ti-75A, respectively. Some samples contained an axial weld seam at the position of maximum applied tensile stress.

5.3.2 Determination of Specimen Deflection

The C-rings were stressed in constant deflection in the usual manner[24], by means of a stainless steel bolt. This was coated with Silastic A RTV to avoid a corrosion couple.

To calculate the deflection corresponding to a prescribed stress, the equation

$$\delta = \frac{\pi D^2}{4EtZ}\ \sigma \tag{4}$$

was utlized in the elastic range. To permit its use at small plastic strains, this is readily converted to

$$\delta = \frac{\pi D^2}{4tZ}\ \epsilon \tag{5}$$

where ϵ is determined from the stress-strain curve at the required stress, and

δ = change of O.D. giving desired stress σ, or strain ϵ,

D = mean diameter,

E = Young's modulus,

t = wall thickness,

Z = constant, f(D/t), evaluated from graph of Ref. 24.

5.4 Testing Temperatures

Stress-corrosion tests were conducted at three temperatures: ambient (75°F), 204°F, and 250°F. In the event of cracking, it had been proposed to expose some coupons at 150°F also, but this was obviated by its absence. In general, the fluctuation in temperature for a single run was a maximum (about $\pm$ 5°F) for the tests at 204°F, a result of the nature of the heating system and control. At room temperature and 250°F the maximum variation observed was $\pm$ 3°F but for a given test was usually much less.

The procedures used to achieve these temperatures are discussed below.

5.5 Velocity Apparatus

Static tests were conducted only at 75°F and 250°F. These were performed simply by immersing the stressed specimens in the saline solutions contained in small glass jars at 75°F, or at 250°F, contained in flasks immersed in distilled water in a pressure vessel subsequently described.

Dynamic tests at 4 and 8 fps were originally planned. The eventual utilization of 4 fps was to be subject to the outcome of test at 0 and 8 fps. The results were such that this intermediate velocity was unnecessary.

To attain a flow velocity of about 8 fps, the bend fixtures were mounted vertically at the periphery of a Teflon wheel, as shown in Figure 2. These were held in place in slots by a thin Teflon strip secured with Teflon screws. Each wheel has positions for 4 bend specimens. This could have been increased to 8 if it had been necessary. However, the general absence of downtime was attributed to the maintenance of a fairly light load. The C-rings were attached to the wheels simply by passing the stressing bolt through a hole near the periphery of the disc.

Each impeller, with a shaft consisting of a drill rod core within 0.5 in. O.D. Teflon tubing, could be revolved at such a rate, through a series of pulleys coupled to the shaft of a 1 HP, 1725 RPM motor, that the linear velocity at the periphery was 8.5 fps. An exchange of pulleys would have yielded 4.25 fps with no difficulty.

The impeller-specimen assembly was immersed in a prescribed solution contained in a 4-1/2 gallon Pyrex jar. A lid in the form of a plexiglass plate reduced evaporation losses at 75°F. At 204°F, condenser lids made of plexiglass were used (Figure 3). A set of plastic (GSC, a glass-silicone laminate) baffle plates served to maintain an average solution velocity of zero (Figure 4).

To attain 204°F, the Pyrex vessels were immersed in a hot air chamber heated electrically by four sets of bar elements. The arrangement is shown in Figure 5.

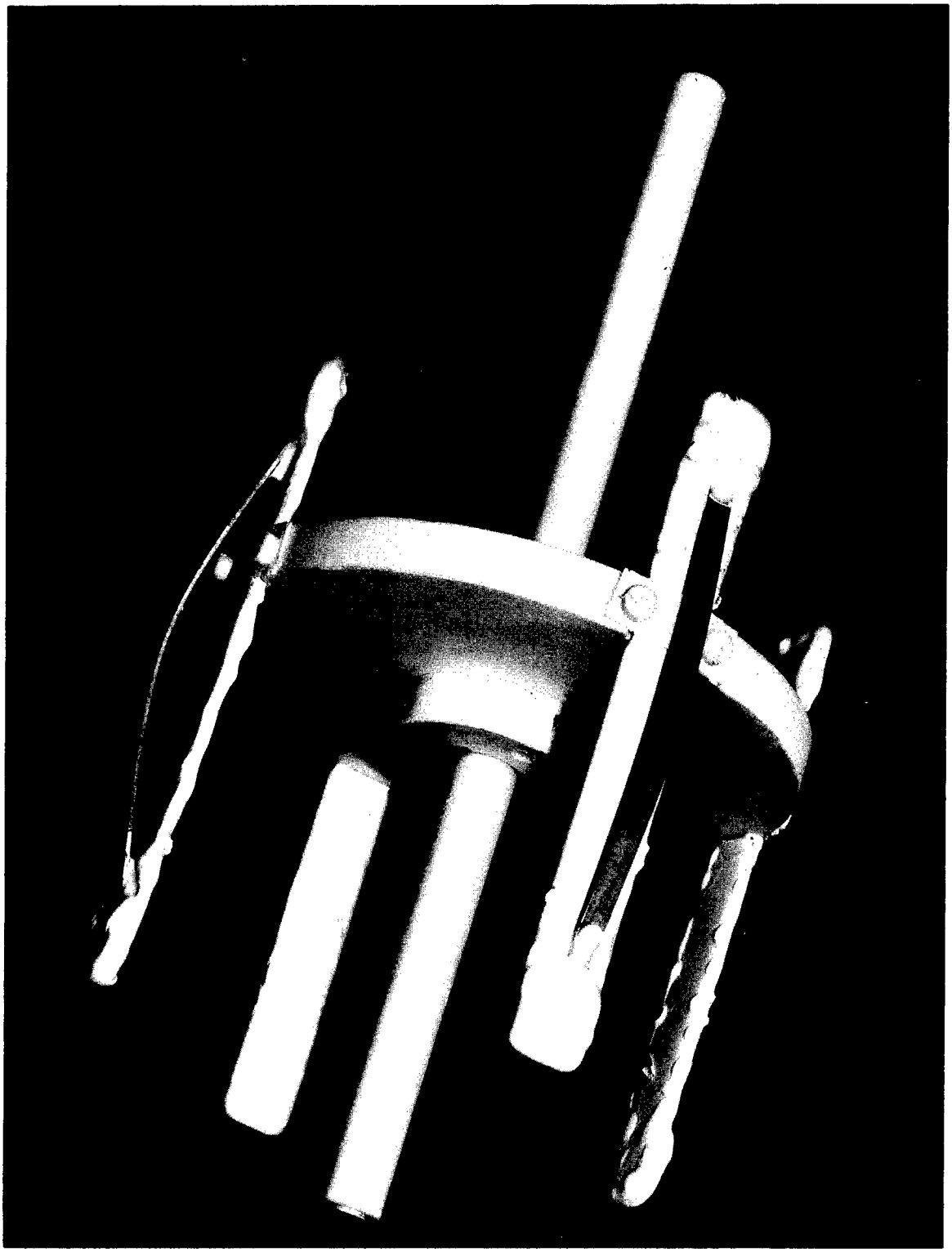

Figure 2. Coated Bend Fixtures Mounted on Teflon Impeller

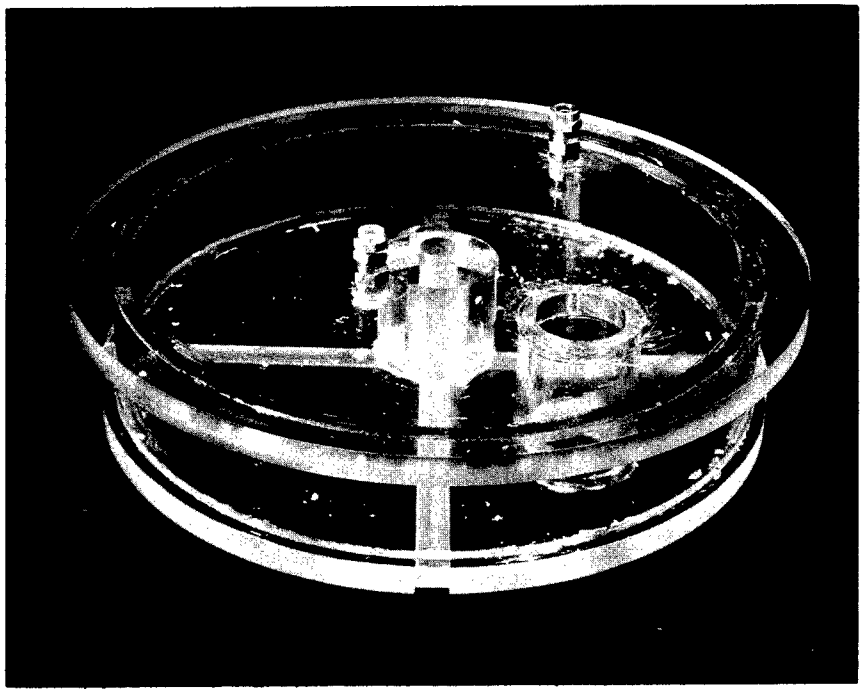

Figure 3. Condenser Lid Used to Cover Pyrex Test Vessels at 204°F

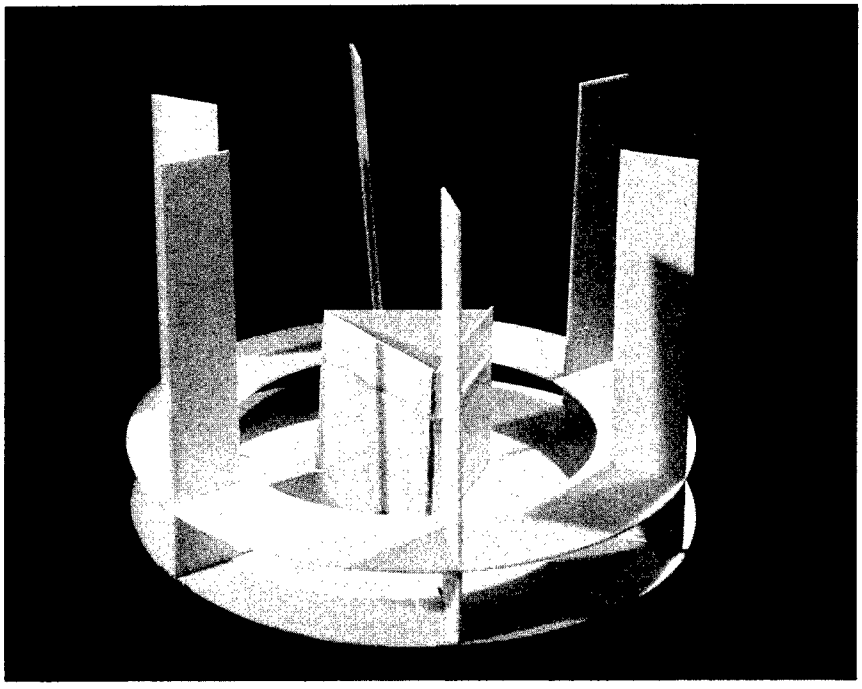

Figure 4. GSC Baffle Plates

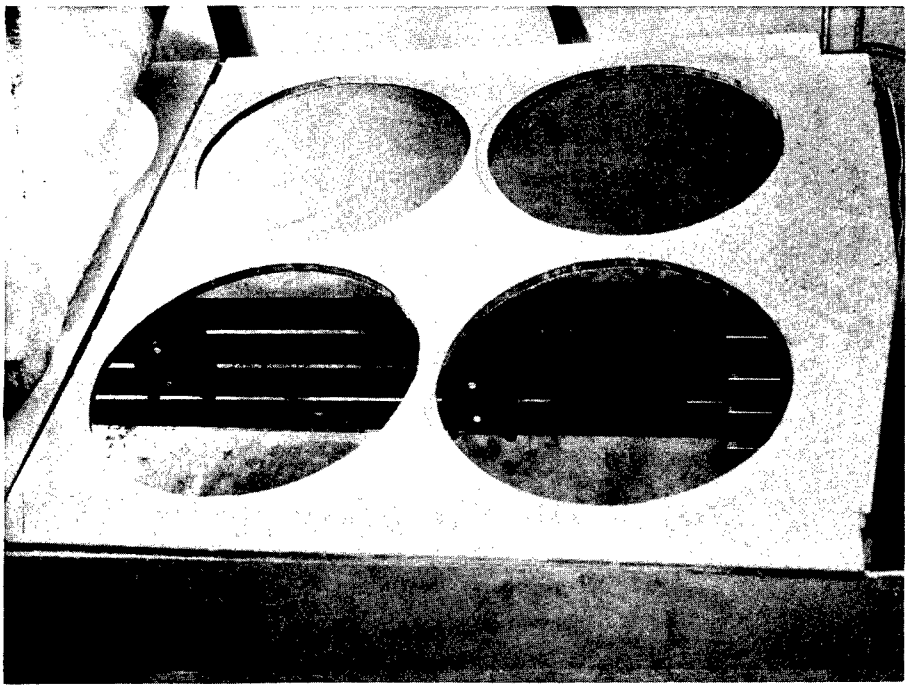

a

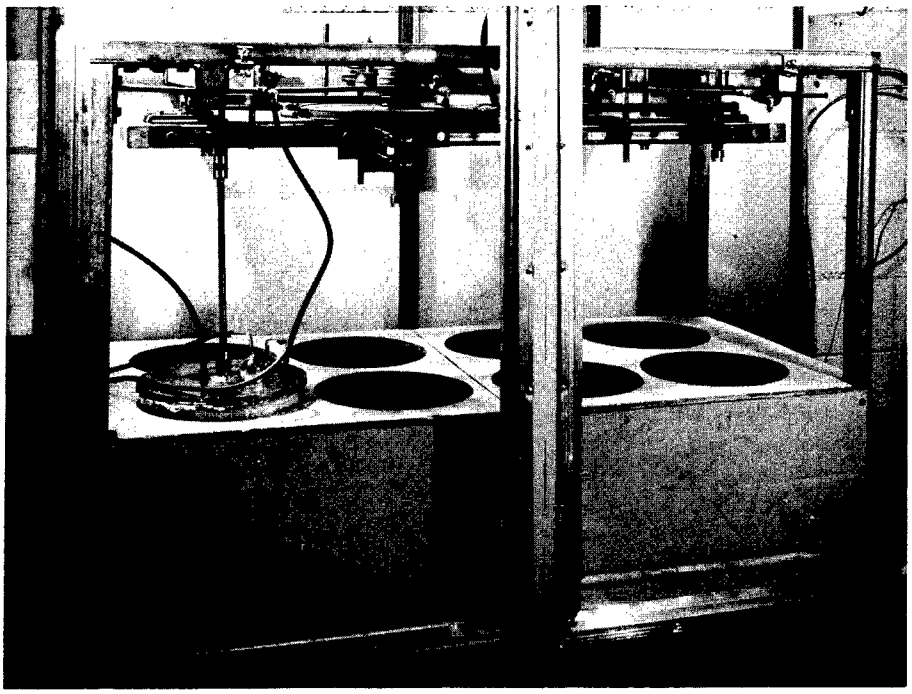

b

Figure 5. Arrangement of Heating Elements and Test Vessels in Hot Air Chamber

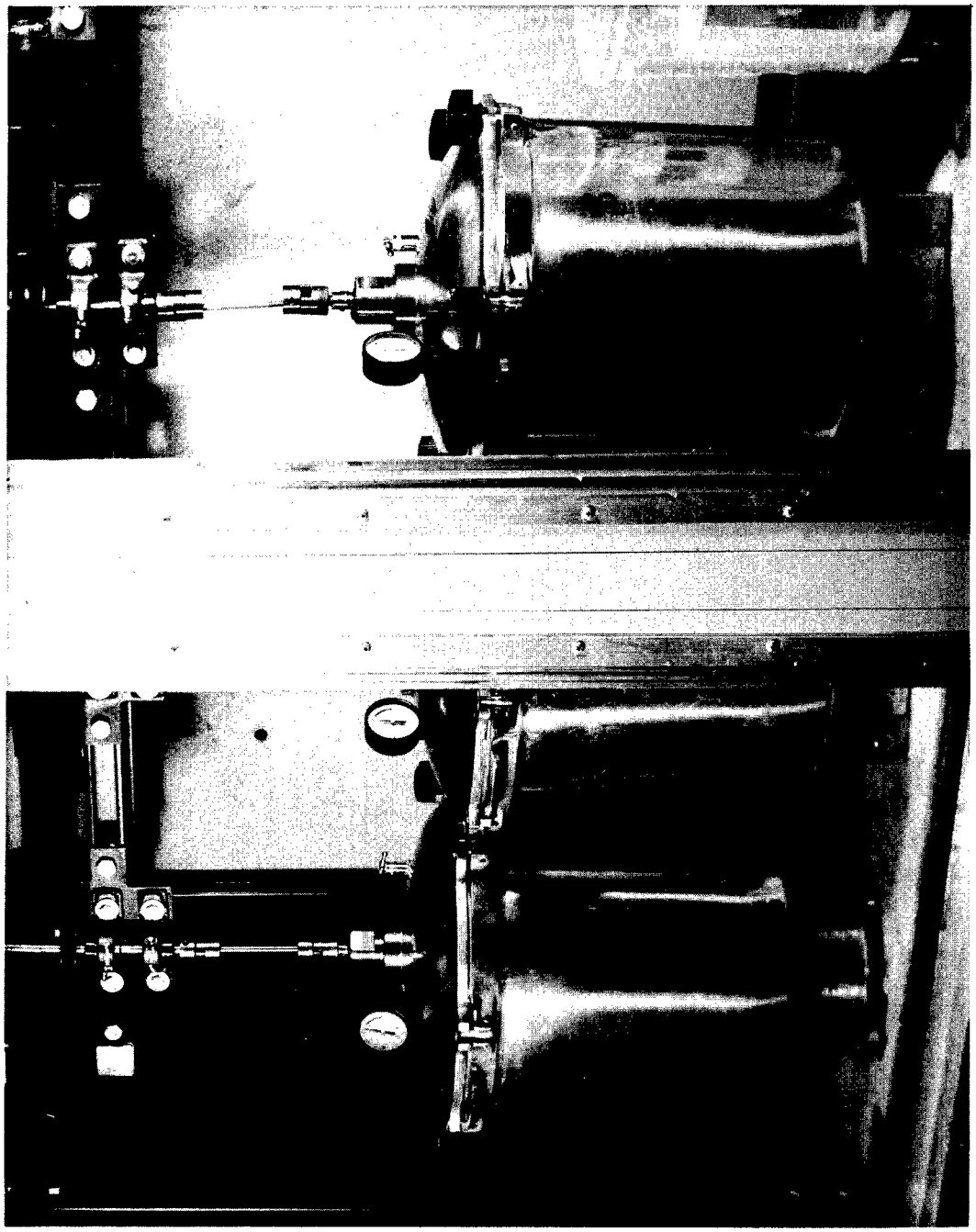

Figure 6. Pressure Vessels Used for Stress Corrosion Tests at 250°F

6. EXPERIMENTAL RESULTS

6.1 Stress Corrosion

In no instance did a stress corrosion failure occur, or were any stress corrosion cracks observed, in Cu-Ni and Ti sheet and tubing for the testing conditions and exposure times detailed in Tables 12 to 15.

6.2 Corrosion

In contrast to the absence of stress corrosion cracking, 90Cu-10Ni and 70Cu-30Ni experienced appreciable material loss by corrosive action for certain exposure conditions. On the other hand, Ti did not exhibit any detectable damage under any circumstances.

Before proceeding to the presentation of the Cu-Ni results, it is necessary to establish the method by which the corrosion rates were determined. Since it was not the primary objective of the program to generate corrosion data, very few of the specimens were weighed prior to exposure. Accordingly, the following procedure was adopted. Firstly, the surface oxide was removed in dilute HCl and the specimen thickness measured to yield dimensionally some information on uniform corrosion. Secondly, the surface was examined for pitting and the average pit depth measured. For conveneince, a "pitting rate" was established. This merely constitutes a standardization to one year of the metal penetration over the exposure period i.e., average pit depth multiplied by the ratio 365/exposure period in days. Lastly, to obtain an average corrosion rate, based on weight loss, the stress corrosion coupons were weighed after exposure and descaling, and the result compared with the average weight of several unexposed specimens of the same length. It was found that this yielded a source of error in evaluating the corrosion rate of less than 1% due to the accuracy demanded in machining the samples.

Thus, the corrosion rates are given as mg. loss per square decimeter per day (mdd), converted in the usual way to mils per year (mpy), for average corrosion, and as mpy for the pitting tendency. In addition, a pitting factor was also calculated which reflects the uniformity of attack. This is the ratio of the rate by pitting (deepest metal penetration) to the rate from weight loss measurements (average metal penetration). A value of unity represents uniform attack.

TABLE 12. Conditions and Accumulated Times for Stress Corrosion Tests of Sheet Material at Room Temperature

Solution	Material	Stress σ/σ_y	Velocity (fps)	Accumulated Testing Time hr.	days
		(a) Unaerated			
Brackish Water	90Cu-10Ni	0.99	0	8307	346
		0.99	8.5	1020	43
	70Cu-30Ni	0.97	0	8283	345
		0.97	8.5	1081	45
	Ti-50A	0.91	0	8311	346
		0.91	8.5	1238	51
		0.75	8.5	1238	51
	Ti-75A	0.91	0	8311	346
		0.91	8.5	1238	51
		0.76	8.5	1238	51
Seawater	90Cu-10Ni	0.90	8.5	1170	49
	70Cu-30Ni	0.90	8.5	1170	49
7% Brine	90Cu-10Ni	0.90	8.5	1176	49
	70Cu-30Ni	0.90	8.5	1176	49
11% Brine	90Cu-10Ni	0.99	0	7441	310
		0.99	8.5	1176	49
		0.90	8.5	1176	49
	70Cu-30Ni	0.97	0	7441	310
		0.97	8.5	1128	47
		0.90	8.5	1128	47
	Ti-50A	0.91	0	7446	310
		0.91	8.5	1191	50
		0.75	8.5	1191	50
	Ti-75A	0.91	0	7446	310
		0.91	8.5	1191	50
		0.76	8.5	1191	50
		(b) Deaerated			
11% Brine	90Cu-10Ni	0.99	0	1176	49
	70Cu-30Ni	0.97	0	1176	49
		(c) Aerated			
11% Brine	90Cu-10Ni	0.99	0	3818	159
	70Cu-30Ni	0.97	0	3818	159

TABLE 13. Conditions and Accumulated Times for Stress Corrosion Tests of Sheet Material at 204°F and 8.5 fps

Solution	Material	Stress* σ/σ_y	Stress* $\sigma(T)/\sigma_y(T)$	Accumulated Testing Time hr.	Accumulated Testing Time days
		(a) Unaerated			
Brackish Water	90Cu-10Ni	0.99	0.99	1128	47
		0.90	0.90	1128	47
	70Cu-30Ni	0.97	0.97	1264	53
	Ti-50A	0.91	1.00	1105	46
		0.75	0.83	1105	46
	Ti-75A	0.91	1.02	1105	46
		0.76	0.98	1105	46
7% Brine	90Cu-10Ni	0.90	0.90	1008	42
	70Cu-30Ni	0.90	0.90	1008	42
11% Brine	90Cu-10Ni	0.99	0.99	1176	49
		0.90	0.90	1176	49
	70Cu-30Ni	0.97	0.97	1128	47
		0.90	0.90	1128	47
	Ti-50A	0.91	1.00	1368	57
		0.75	0.83	1368	57
	Ti-75A	0.91	1.02	1368	57
		0.76	0.98	1368	57
		(b) Deaerated			
11% Brine	90Cu-10Ni	0.99	0.99	1176	49
	70Cu-30Ni	0.97	0.97	1128	47

* σ/σ_y is the ratio of the stress applied at room temperature to the room-temperature yield stress; $\sigma(T)/\sigma_y(T)$ is the ratio of the operative stress at elevated temperature, T, to the elevated-temperature yield stress.

TABLE 14. Conditions and Accumulated Times for Stress Corrosion Tests of Sheet Material at 250°F

Solution	Material	Stress σ/σ_y	Stress $\sigma(T)/\sigma_y(T)$	Velocity (fps)	Accumulated Testing Time hr.	Accumulated Testing Time days
Brackish Water	90Cu-10Ni	0.99	0.99	0	1464	61
		0.99	0.99	8.5	1472	61
	90Cu-10Ni (cold-rolled 50%)	1.00	1.00	0	1008	42
		1.00	1.00	8.5	998	42
	70Cu-30Ni	0.97	0.97	0	1464	61
		0.97	0.97	8.5	1056	44
	70Cu-30Ni (cold-rolled 50%)	1.00	1.00	0	1008	42
		1.00	1.00	8.5	1056	44
	Ti-50A	0.91	1.03	0	1464	61
		0.91	1.03	8.5	1008	42
	Ti-75A	0.91	1.04	0	1464	61
		0.91	1.04	8.5	1008	42
	Ti-75A (cold-rolled 40%)	1.00	1.31	0	1008	42
		1.00	1.31	8.5	1008	42
11% Brine	90Cu-10Ni	0.99	0.99	0	1046	43
		0.99	0.99	8.5	1032	43
	90Cu-10Ni (cold-rolled 50%)	1.00	1.00	0	1008	42
		1.00	1.00	8.5	1032	43
	70Cu-30Ni	0.97	0.97	0	1046	43
		0.97	0.97	8.5	1008	42
	70Cu-30Ni (cold-rolled 50%)	1.00	1.00	0	1008	42
		1.00	1.00	8.5	1008	42
	Ti-50A	0.91	1.03	0	1046	43
		0.75	0.90	0	1046	43
		0.91	1.03	8.5	1008	42
	Ti-50A (cold-rolled 40%)	1.00	1.15	0	1008	42
		1.00	1.15	8.5	1056	44
	Ti-75A	0.91	1.04	0	1046	43
		0.76	1.00	0	1046	43
		0.91	1.04	8.5	1008	42
	Ti-75A (cold-rolled 40%)	1.00	1.31	0	1008	42
		1.00	1.31	8.5	1056	44

TABLE 15. Conditions and Accumulated Testing Times for Stress Corrosion Tests of Tubing

Solution	Material	Specimen Configuration*	Stress σ/σ_y	Stress $\sigma(T)/\sigma_y(T)$	Velocity (fps)	Accumulated Testing Time hr.	Accumulated Testing Time days
			(a) 204 °F				
11% Brine	90Cu-10Ni	C-ring (S)	0.99	0.99	8.5	1008	42
		C-ring (W)	0.99	0.99	8.5	1008	42
		Longit. (S)	0.99	0.99	8.5	1008	42
			(b) 250 °F				
Brackish Water	90Cu-10Ni	C-ring (S)	0.99	0.99	0	1176	49
		C-ring (W)	0.99	0.99	0	1176	49
		Longit. (S)	0.99	0.99	0	1176	49
		Longit. (W)	0.99	0.99	0	1176	49
		C-ring (S)	0.99	0.99	8.5	1160	48
		C-ring (W)	0.99	0.99	8.5	1160	48
		Longit. (S)	0.99	0.99	8.5	998	42
	70Cu-30Ni	C-ring (S)	0.99	0.99	0	1176	49
		Longit. (S)	0.99	0.99	0	1176	49
		C-ring (S)	0.99	0.99	8.5	1056	44
		Longit. (S)	0.99	0.99	8.5	1056	44
	Ti-50A	C-ring (S)	0.90	1.02	0	1176	49
		Longit. (S)	0.90	1.02	0	1176	49
		C-ring (S)	0.90	1.02	8.5	1008	42
		Longit. (S)	0.90	1.02	8.5	1008	42
	Ti-75A	C-ring (S)	0.90	1.03	0	1176	49
		C-ring (W)	0.90	1.03	0	1176	49
		Longit. (S)	0.90	1.03	0	1176	49
		Longit. (W)	0.90	1.03	0	1176	49
		C-ring (S)	0.90	1.03	8.5	1008	42
		C-ring (W)	0.90	1.03	8.5	1008	42
		Longit. (S)	0.90	1.03	8.5	1008	42
11% Brine	90Cu-10Ni	C-ring (S)	0.99	0.99	0	1008	42
		C-ring (W)	0.99	0.99	0	1008	42
		Longit. (S)	0.99	0.99	0	1008	42
		Longit. (W)	0.99	0.99	0	1008	42
		C-ring (S)	0.99	0.99	8.5	1032	43
		C-ring (W)	0.99	0.99	8.5	1032	43
		Longit. (S)	0.99	0.99	8.5	1032	43
	70Cu-30Ni	C-ring (S)	0.99	0.99	0	1008	42
		Longit. (S)	0.99	0.99	0	1008	42
		C-ring (S)	0.99	0.99	8.5	1008	42
		Longit. (S)	0.99	0.99	8.5	1008	42
	Ti-50A	C-ring (S)	0.90	1.02	0	1008	42
		Longit. (S)	0.90	1.02	0	1008	42
		C-ring (S)	0.90	1.02	8.5	1056	44
		Longit. (S)	0.90	1.02	8.5	1056	44
	Ti-75A	C-ring (S)	0.90	1.03	0	1008	42
		C-ring (W)	0.90	1.03	0	1008	42
		Longit. (S)	0.90	1.03	0	1008	42
		C-ring (S)	0.90	1.03	8.5	1008	42
		C-ring (W)	0.90	1.03	8.5	1008	42
		Longit. (S)	0.90	1.03	8.5	1008	42
		Longit. (W)	0.90	1.03	8.5	1056	44

* (S) denotes seamless specimens and (W) those with a weld seam.

Some corrosion of Cu-Ni sheet occurred in 11% brine and brackish well water after nearly one year of static exposure at ambient temperature. The corrosion rates were very low, of the order of 0.3 mpy, as shown in Table 16. The pitting factor of 6 for 90Cu-10Ni in brackish water resulted from a single pit.

Shorter term static exposures in either brackish water or 11% brine did not result in any detectable loss of material. Moreover, no corrosive attack was measurable from stress corrosion specimens subjected to 8.5 fps in brackish water at 75, 204, or 250°F.

However, a velocity of 8.5 fps, in conjunction with exposure to seawater and sea-salt brines resulted in damage, in many cases severe, to both Cu-Ni alloys. The corrosion rates are tabulated in Table 16.

At 75 and 204°F, it was found that an increase in the total salt content increased the corrosion rate, as illustrated in Figures 7 and 8. For example, as contrasted to less than 1 mpy in San Diego Bay water (4% salt), a maximum average rate of ~40 mpy (70Cu-30Ni, 204°F) and a maximum pitting rate of nearly 200 mpy (90Cu-10Ni, 204°F) were obtained in 11% brine.

An increase in the exposure temperature apparently reduces the average corrosion rate in 7% and 11% brine (Figure 9). The exception was 70Cu-30Ni which, when tested in 11% brine, displayed the greatest deterioration at 204°F. The pitting rates of 90Cu-10Ni and 70Cu-30Ni in 11% brine were also highest at 204°F (Figure 10). On the other hand, in 7% brine the temperature dependence of the pitting rates more closely paralleled that of the average rates.

It is recognized that the utilization of two or three data points per curve in the figures establishes a trend only and is not to be misconstrued as being indicative of rigorous behavior.

As seen from Table 16, Section C, the corrosion rates for tubing agree reasonably well with those for sheet material except in two instances. The average rate for 90Cu-10Ni at 250°F was 6 times greater for tubing than for sheet, although the degree of attack remained relatively low. Alternatively, 90Cu-10Ni sheet appeared to be about 10 times more susceptible to pitting at 204°F than tubing.

It is noteworthy that the aeration or deaeration of 11% brine did not result in any corrosion in a static test at 75°F. Aeration was

TABLE 16. Corrosion Rates for Cu-Ni Alloys

Alloy	Corrodent (a)	Temperature (°F)	Exposure Time (days)	Corrosion Rates: Weight Loss (mdd)	Corrosion Rates: Weight Loss (mpy)	Pitting (mpy)	Pitting Factor
			(a) Sheet; Static				
90Cu-10Ni	B.W., unaerated	75	346	1.6	0.3	1.8	6.0
	11%, unaerated	75	310	2.0	0.3	0.2	1.0
70Cu-30Ni	B.W., unaerated	75	345	1.3	0.2	0	1.0
	11%, unaerated	75	310	0.9	0.2	0.4	2.0
			(b) Sheet; 8.5 fps				
90Cu-10Ni	S.W., unaerated	75	49	2.3	0.4	0	1.0
	7%, unaerated	75	49	27.7	4.5	22.6	5.0
		204	42	5.4	0.9	22.9	25.4
	11%, unaerated	75	49	169	27.1(b)	37.2	1.4
		204	49	78.7	12.7	191	15.0
		250	43	6.8	1.1	18.0	16.4
	11%, deaerated	204	49	170	27.3	80.8	3.0
90Cu-10Ni (cold-rolled 50%)	11%, unaerated	250	43	25.7	4.1	9.3	2.3
70Cu-30Ni	S.W., unaerated	75	49	6.3	1.0	0	1.0
	7%, unaerated	75	49	29.3	4.7	19.4	4.1
		204	42	0	0	0	1.0
	11%, unaerated	75	47	108	17.3	83.2	4.8
		204	47	260	41.7	98.7	2.4
		250	42	51.7	8.3	8.7	1.0
	11%, deaerated	204	47	24.7	4.0	62.3	15.6
70Cu-30Ni (cold-rolled 50%)	11%, unaerated	250	42	54.2	8.7	5.7	1.0
			(c) Tubing; 8.5 fps				
90Cu-10Ni	11%, unaerated	204	42	95.3	15.3	21.9	1.4
		250	43	41.0	6.6	13.3	2.0
70Cu-30Ni	11%, unaerated	250	42	41.0	6.6	5.2	1.0

(a) B.W.: brackish well water from Roswell, N.M.
S.W.: San Diego Bay seawater (4% total salt).
7%: 7% sea-salt brine from San Diego Test Facility.
11%: 11% sea-salt brine prepared from 7% brine.

(b) Corrosion rate from corrosion coupons = 19.2 mpy.

DENVER RESEARCH INSTITUTE — UNIVERSITY OF DENVER

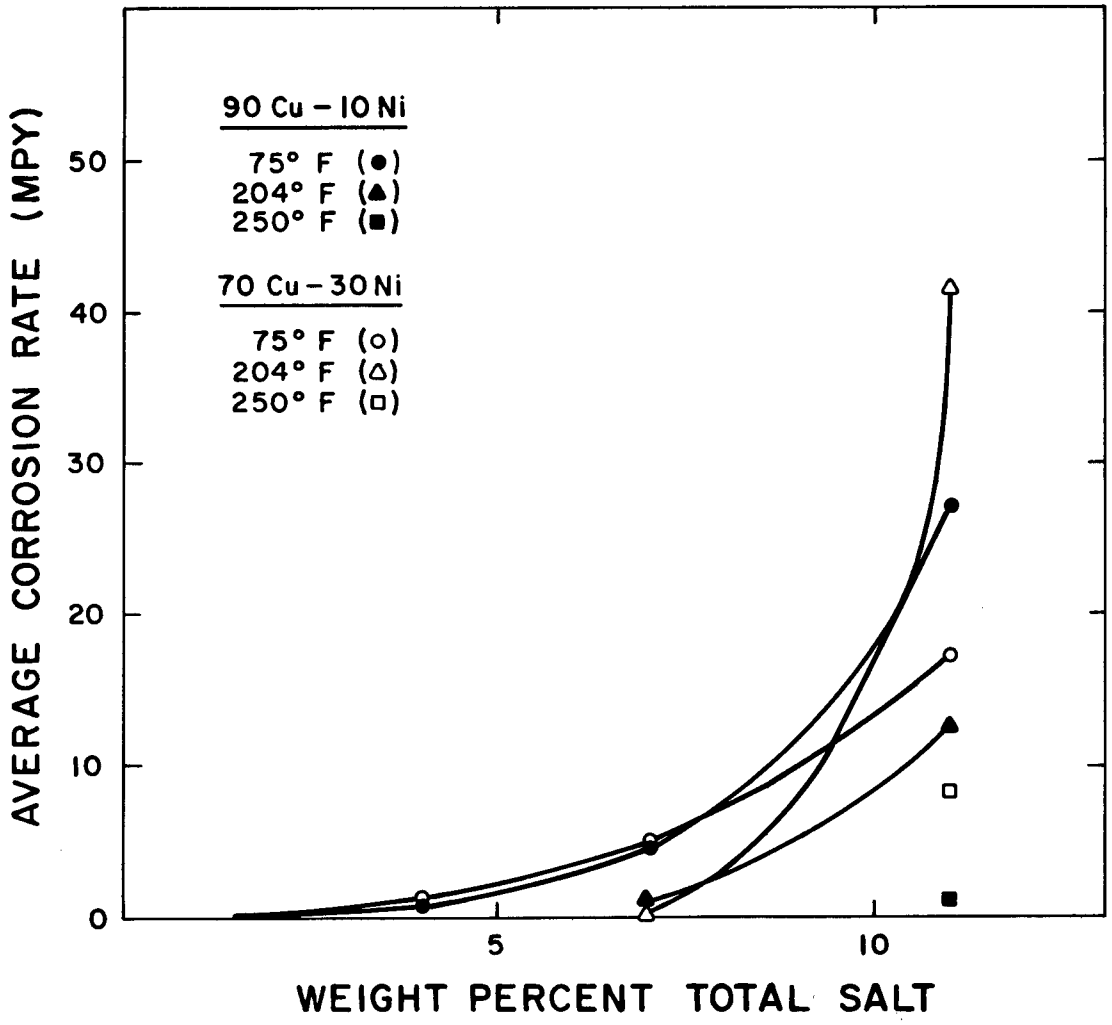

Figure 7. Effect of Total Salt Content of Corrodent on the Average Corrosion Rate of Cu-Ni Sheet Tested at 8.5 fps

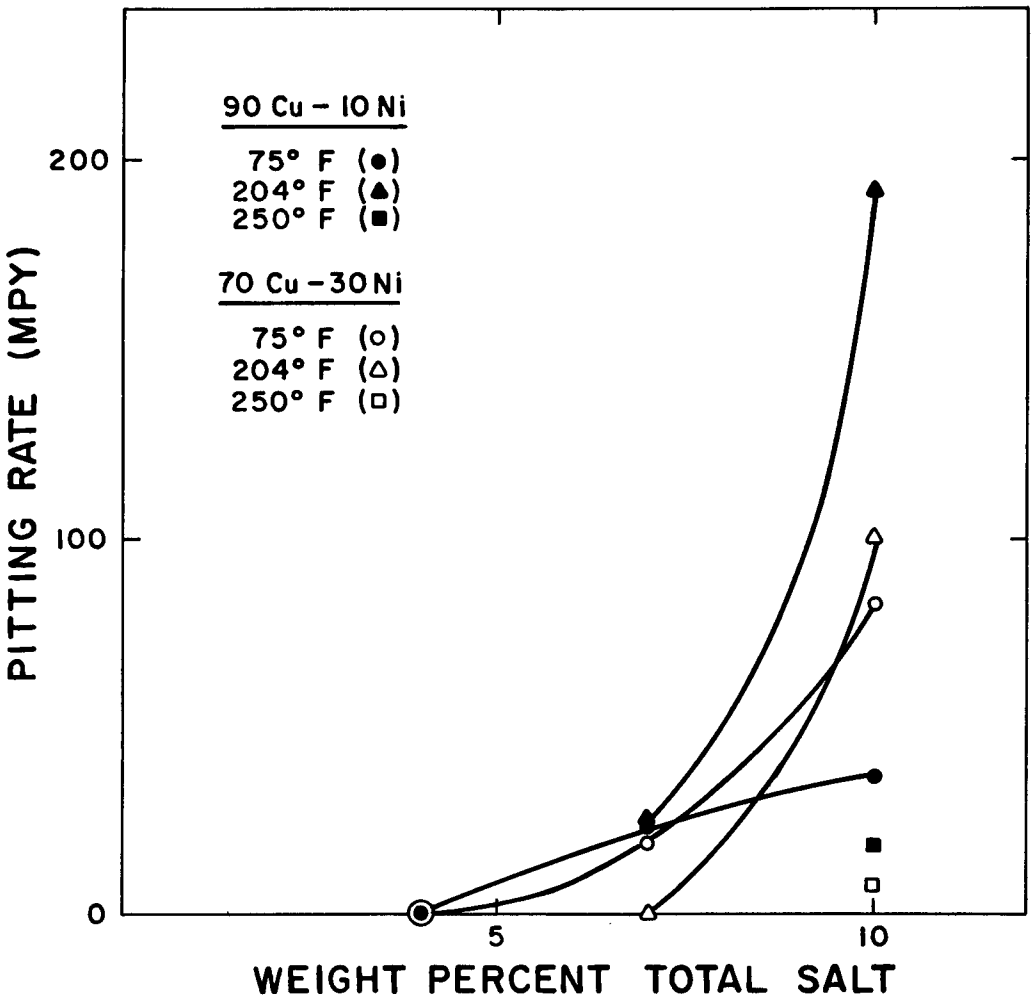

Figure 8. Effect of Total Salt Content of Corrodent on the Pitting Rate of Cu-Ni Sheet Tested at 8.5 fps

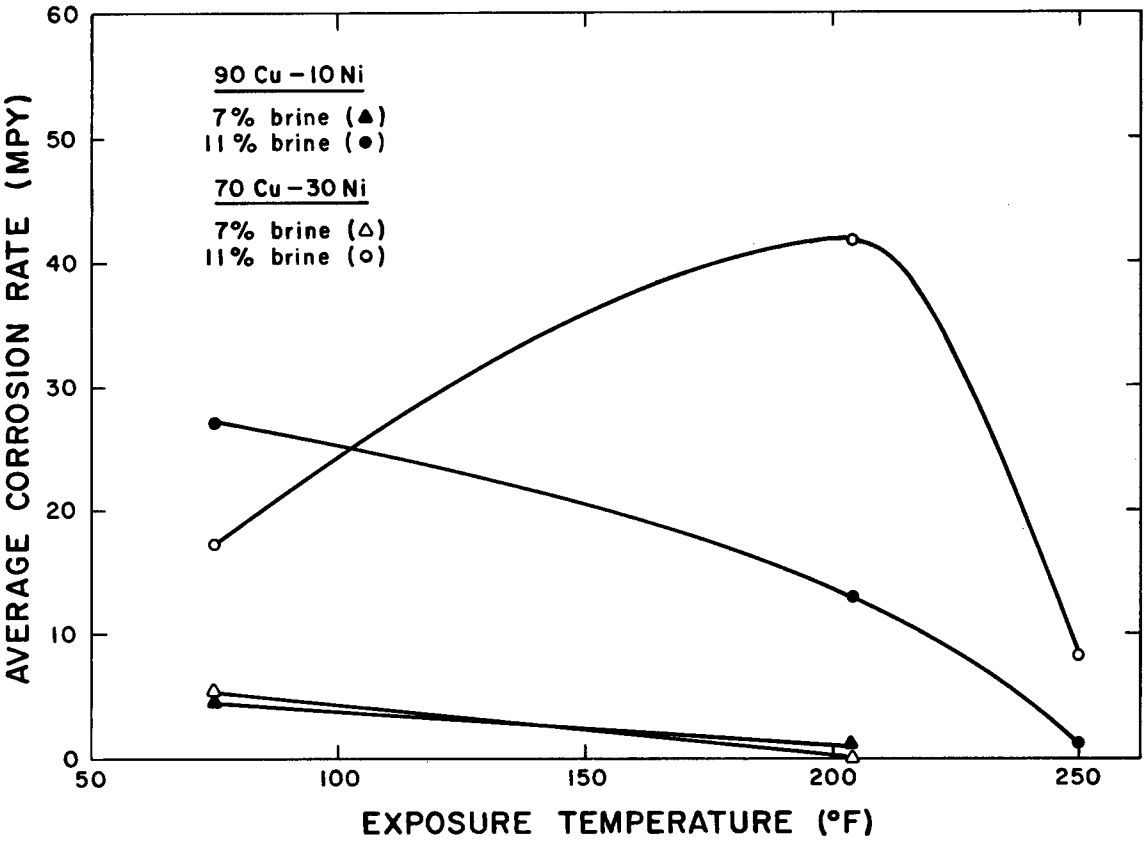

Figure 9. Effect of Exposure Temperature on the Average Corrosion Rate of Cu-Ni Sheet Tested at 8.5 fps

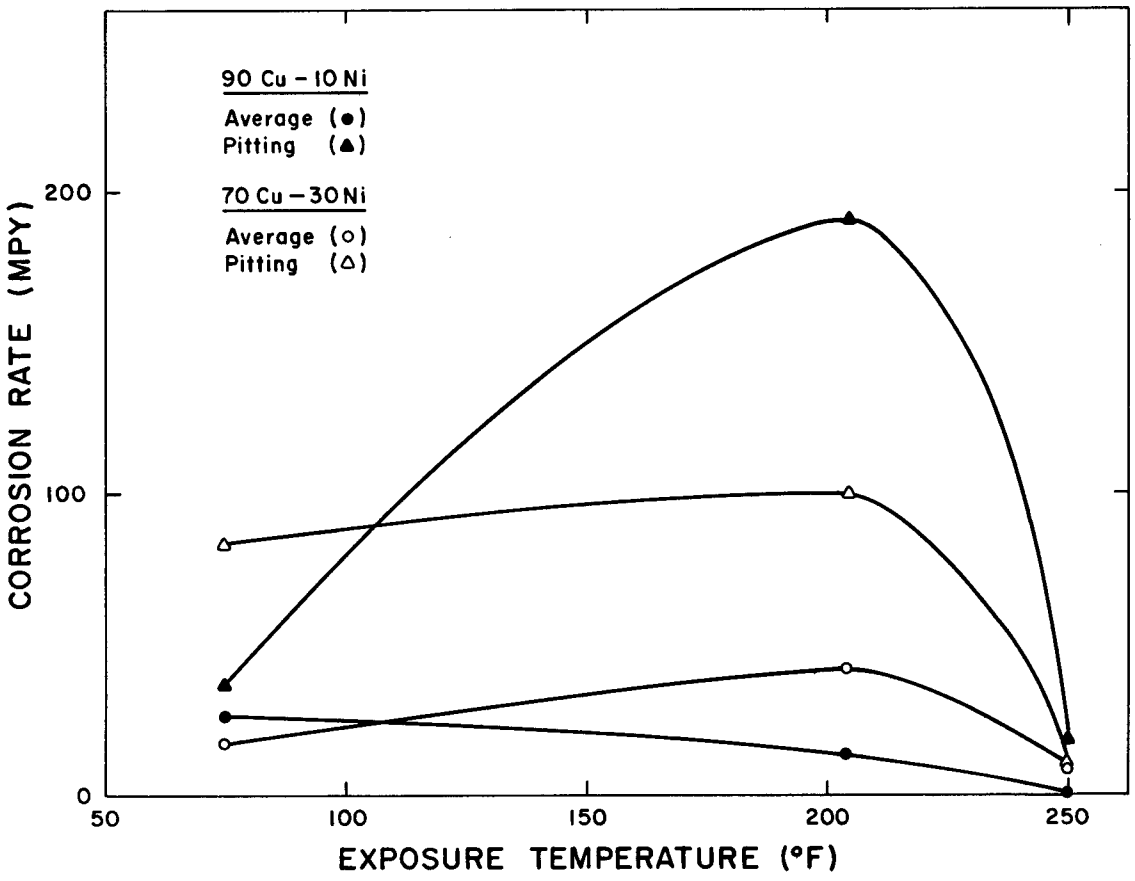

Figure 10. Comparison of Average Corrosion and Pitting Rates of Cu-Ni Sheet Tested at 8.5 fps in 11% Sea-Salt Brine

effected by bubbling air through the solutions, and deaeration similarly, using nitrogen gas. Deaeration of 11% brine at 204°F did increase the corrosion rate of 90Cu-10Ni at 8.5 fps and reduced the rate of 70Cu-30Ni (Table 16).

In order to confirm that the corrosion rates evaluated from the stress corrosion specimens were reasonably valid, some corrosion coupons (3 in. × 0.5 in. × 0.05 in.) of 90Cu-10Ni were run at 8 to 10 fps in 11% brine at room temperature. This test was performed with the cooperation of Dr. D. T. Klodt of this laboratory who was responsible for an investigation of the effects of velocity on the passivation of alloys in brackish water for the Office of Saline Water (Contract No. 14-01-0001-1335). After exposure for the same period (49 days) as the stress corrosion samples, an average corrosion rate of 19.2 mpy was obtained from weight-loss measurements. This is about two-thirds of that (27.1 mpy) obtained by the other method. This difference in the average rate is attributable to the less uniform attack of the corrosion coupons, as manifested in Figure 11. The surface appearance of 90Cu-10Ni stress corrosion specimens tested at 8.5 fps in 11% brine at room temperature is shown in Figure 12 for comparison. In turn, the uniformity of attack could be due to the specimen size difference, and also to its position relative to the Teflon impeller and flow direction.

Other examples of the result of dynamic exposure to the brine solutions are given in Figures 13 to 18. In general, corrosion pits were somewhat more numerous in that region of the surface near the leading edge of the specimens, and near the ends of the specimens where the RTV coating terminates. Rather than a crevice effect, the latter is thought to be the result of excessive turbulence at the specimen-fixture junctions since the C-rings did not experience similar effects (Figure 15).

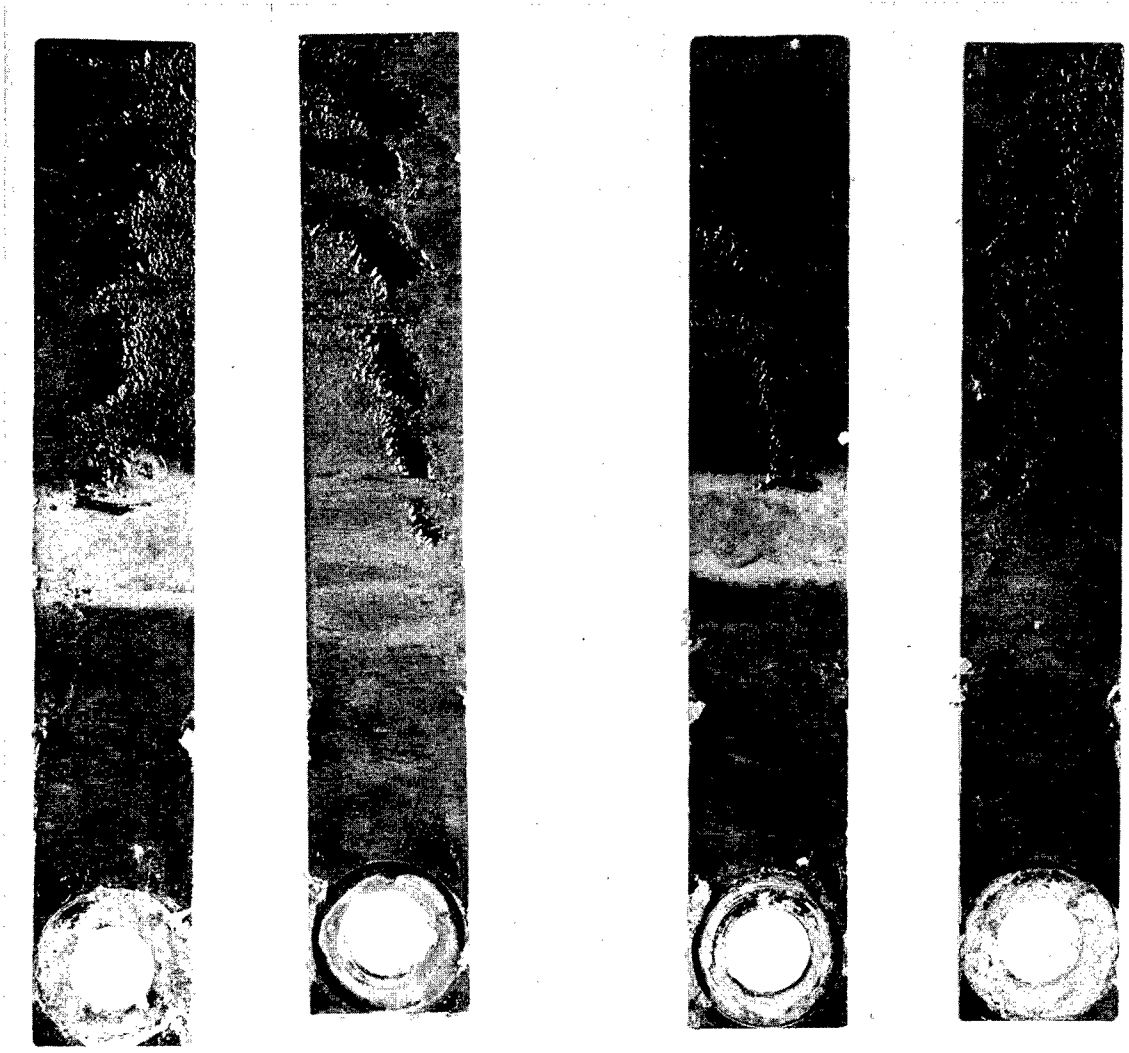

Figure 11. Surface Appearance of Typical 90Cu-10Ni Corrosion Coupons Exposed for 49 Days at 8 to 10 fps in 11% Sea-Salt Brine at Room Temperature

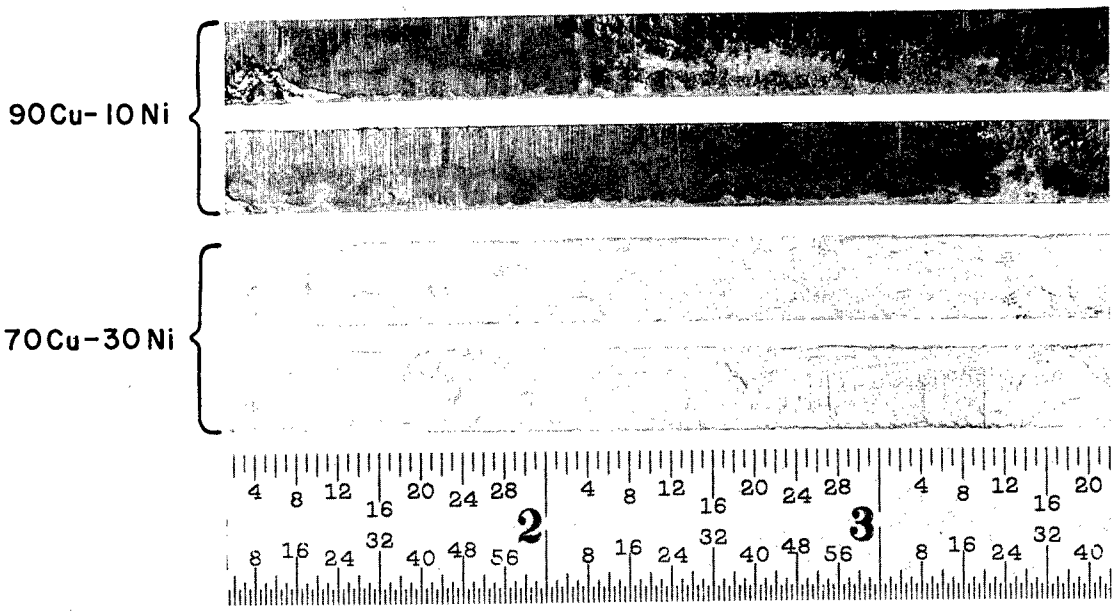

Figure 12. Surface Appearance of 90Cu-10Ni and 70Cu-30Ni Stress Corrosion Specimens Exposed for 49 and 47 Days, Respectively, at 8.5 fps in 11% Sea-Salt Brine at Room Temperature

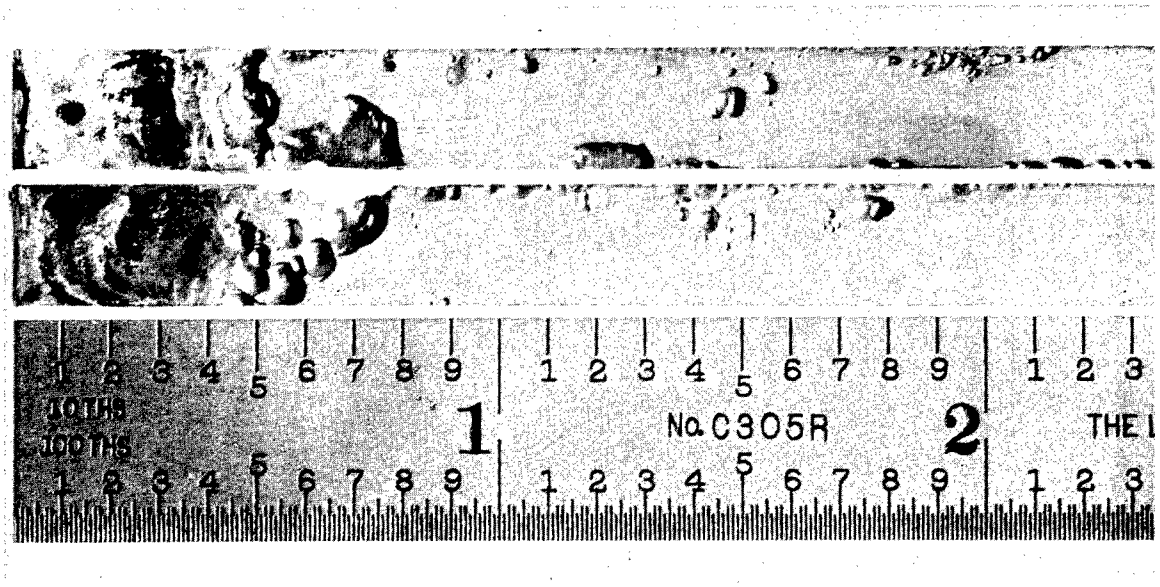

Figure 13. Surface Appearance of 90Cu-10Ni Stress Corrosion Specimens Exposed for 49 Days at 8.5 fps in 11% Sea-Salt Brine at 204°F

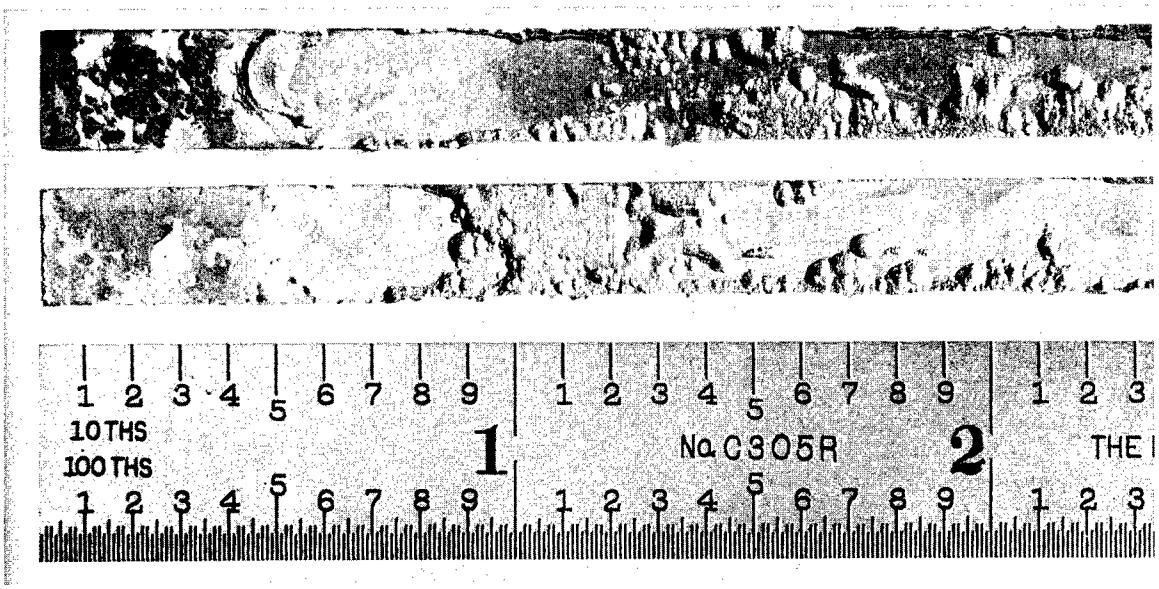

Figure 14. Surface Appearance of 70Cu-30Ni Stress Corrosion Specimens Exposed for 47 Days at 8.5 fps in 11% Sea-Salt Brine at 204°F

Figure 15. Surface Appearance of 90Cu-10Ni Tube Specimens Exposed for 42 Days at 8.5 fps in 11% Sea-Salt Brine at 204°F. Top Left: Seamless C-Ring; Top Right: C-Ring with Weld Seam; Bottom: Longitudinal Bent-Beam

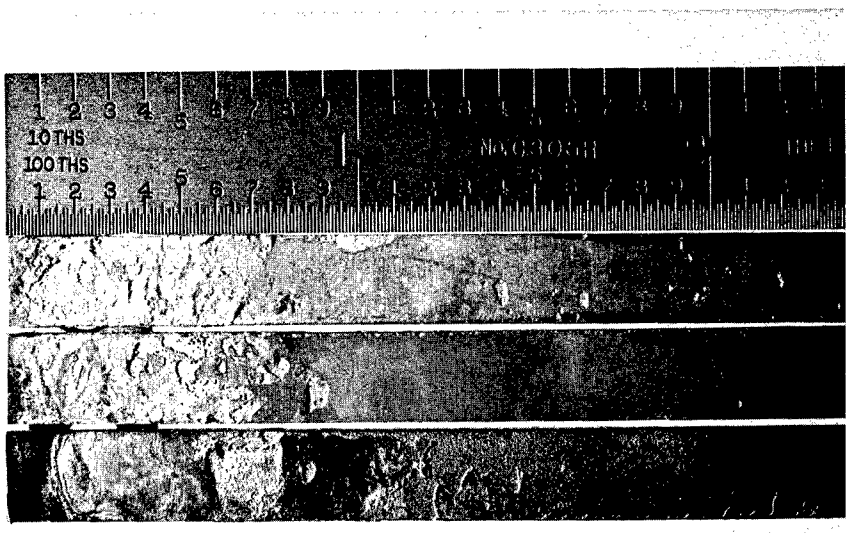

Figure 16. Surface Appearance of 90Cu-10Ni Exposed for 43 Days in 11% Sea-Salt Brine at 250°F. Top: Sheet Cold-Rolled 50%; Center: Annealed Sheet; Bottom: Longitudinal Tube

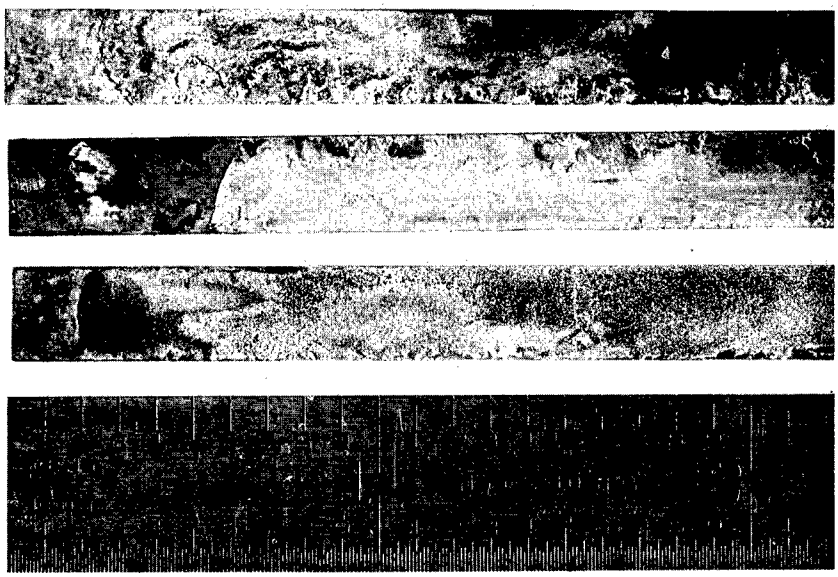

Figure 17. Surface Appearance of 70Cu-30Ni Exposed for 42 Days in 11% Sea-Salt Brine at 250°F. Top: Sheet Cold-Rolled 50%; Center: Longitudinal Tube; Bottom: Annealed Sheet

Figure 18. Surface Appearance of 90Cu-10Ni (Top) and 70Cu-30Ni (Bottom) Exposed for 49 Days in 7% Sea-Salt Brine at Room Temperature

7. DISCUSSION AND CONCLUSIONS

7.1 Stress Corrosion

In general, it can be concluded from the results of this laboratory investigation together with service experience[6], that stress corrosion cracking is extremely unlikely to be the cause of failure of 90Cu-10Ni, 70Cu-30Ni, or unalloyed Ti tubes or tube sheets in desalination plants.

More specifically, these two Cu-Ni alloys, and 50A and 75A Ti, are not susceptible to stress corrosion cracking under the following conditions:

1. in static unaerated brackish well water from Roswell, N.M., at 75 and 250°F;
2. in brackish water flowing at 8.5 fps at 75, 204, and 250°F;
3. in unaerated natural seawater flowing at 8.5 fps at 75°F;
4. in unaerated sea-salt brine containing 7 w/o total salt, flowing at 8.5 fps at 75 and 204°F;
5. in static unaerated sea-salt brine containing 11 w/o total salt, at 75 and 250°F;
6. in unaerated 11% brine flowing at 8.5 fps at 75, 204, and 250°F.

In addition, Cu-Ni is not susceptible in static deaerated or aerated 11% brine at 75°F, and in deaerated 11% brine flowing at 8.5 fps at 204°F.

It should be borne in mind that these conclusions are based on exposure periods of about 40 to 50 days only, but at the same time, at applied stresses very close to or just in excess of the macroscopic yield stress. Moreover, the introduction of plastic deformation by cold rolling to 40 to 50% reduction does not induce susceptibility when the materials are tested at the prestrained yield stress.

→ 47

→ p. 47

Therefore, from the standpoint of stress corrosion behavior, one cannot recommend, among 90Cu-10Ni, 70Cu-30Ni, Ti-50A, and Ti-75A, one over the other for desalination service. All are equally satisfactory.

7.2 Corrosion

Unalloyed Ti did not experience any general corrosion during exposures for, or just in excess of, 1000 hr. in brackish well water, seawater, or sea-salt brines with up to 11 w/o salt contents, when static or flowing at 8.5 fps at temperatures up to 250°F. This observation is in agreement with previous findings concerning the corrosion behavior of Ti in saline environments. For example, Feige and Kane[26] reported service and laboratory experience covering periods of 6 months to 2 years wherein no measurable loss of material, or indeed any indication of corrosive attack, was observed. The most severe service condition cited was one which involved a 23% NaCl slurry at 21 fps and 250°F (~ 1-1/2 years' exposure). The results of multi-stage flash distillation plant operation, although limited to one plant to date, confirms the suitability of titanium for desalination service. No tube failures were reported after 26 months of operation[6].

In contrast, flowing sea-salt brines can lead to extremely severe deterioration of 90Cu-10Ni and 70Cu-30Ni even at ambient temperature. Observed penetration rates by pitting indicate that 90Cu-10Ni and 70Cu-30Ni tubing with a wall thickness of 0.05 in. would not be expected to last in excess of 3 and 6 months, respectively, when exposed to unaerated 11% sea-salt brine flowing at 8 to 9 fps near its boiling point. These lifetimes are longer (~ 1 year and 8 months) if the brine temperature were about 75°F. The effects at 250°F are less pronounced, yielding projected lifetimes of about 3 and 6 years, respectively.

The Cu-Ni alloys in general, and 70Cu-30Ni in particular, are considered to exhibit excellent corrosion resistance in static seawater at elevated temperatures (450°F continuous operation) and appear to behave extremely well under dynamic conditions conducive to impingement attack or erosion, up to velocities of 15 fps[27,28]. Desalination service experience confirms these findings. Newton and Birkett[6], in their survey of 55 MSFD plants, discovered that less than 1% of all Cu-Ni tubes had failed in service and that many of these failures could be attributed to bad descaling practice.

The author is unaware of any previous work with which the results of the present investigation can be compared directly. There are some data at the two extremes of the conditions used. For example, Feige and Kane[26] cited weight-loss results for several materials, including 90Cu-10Ni and 70Cu-30Ni, which suggested corrosion rates in 20% salt-brines flowing at 10 fps at 226°F in good agreement with those obtained here. At the other end of the scale, corrosion rates of Cu-Ni in ambient-temperature seawater flowing at 1 to 3 fps can be expected to be 0.3 to 1.0 mpy[27]. In deaerated normal seawater at the Freeport, Texas plant, the average corrosion rates of 90Cu-10Ni and 70Cu-30Ni varied from 4 mpy at 135°F to 0.5 mpy at 250°F[7]. These are higher than were obtained here in unaerated seawater at 75°F. They are also higher than would have been obtained at higher temperatures if the observed negative temperature dependence of the rate maintained (Ref. 7, and Figure 9). Stewart and LaQue[19] performed velocity experiments, also by rotation, in deaerated (air bubbles removed) seawater at 73°F. Corrosion rates for 90Cu-10Ni (1.25 Fe) ranged from 4.0 to 10.4 mpy at 15 fps, and 12.9 to 15.3 mpy at 30 fps, depending upon the fraction of the iron in solution. Similarly, the average corrosion rate of 70Cu-30Ni (0.5Fe) was 6.4 mpy at 15 fps and 12.0 mpy at 30 fps. Consider these rates in relation to the average values from the present work of 0.4 mpy for 90Cu-10Ni and 1.0 mpy for 70Cu-30Ni at 8.5 fps in unaerated seawater at 75°F, and 27.1 and 17.3 mpy, respectively, in unaerated 11% brine. Thus, for the type of test utilized, the results seem to be in accord with former work.

The high corrosion rates obtained in this study relative to those characteristic of actual service conditions are attributable to several factors. Firstly, the amount of oxygen in the present solutions must be considered relatively high. It is doubtful whether the deaeration process in the velocity test with 11% brine at 204°F served any purpose other than to reduce the concentration of air bubbles. According to Stewart and LaQue, [19] this would raise the corrosion rate due to impingement which, in fact, occurred with 90Cu-10Ni. The deaeration in the case of 70Cu-30Ni seemed to have been more effective in reducing the amount of oxygen in solution since the average rate was reduced from 41.7 mpy to 4.0 mpy. Secondly, the solutions were not recirculated, a feature which could substantially increase the concentration of damaging ions in solution. Thirdly, the possibility that the flow in the present circumstances is appreciably more turbulent than in service would intensify impingement action. Lastly, the highest brine concentration used was higher than generally experienced in service. The 7% brine, for example, obtained directly from the San Diego Test Facility, yielded average rates less than 1 mpy at 204°F.

The observed corrosion of Cu-Ni under dynamic conditions is thought to be due almost entirely to impingement action[2, 29]. It is significant that aeration of the 11% brine in a static test at room temperature did not reduce the corrosion resistance from an undetectable level. An increase in the sea-salt concentration beyond 7% produces a rapid enhancement of the corrosive attack. The low corrosion rates at 250°F, subsequent to high values at 204°F are probably the result of a lower dissolved oxygen content in the solutions contained under pressure. It is felt that this further illustrates the importance of the oxygen concentration of the corrodents.

With regard to general corrosion, it seems evident that:

1. titanium does not experience any corrosive attack in flowing sea-salt brines up to temperatures of 250°F;

2. Cu-Ni can suffer appreciable material loss in flowing sea-salt brines (7 to 11 w/o total salt) in the temperature range of 75 to 250°F;

3. the observed corrosion of Cu-Ni is an impingement effect;

4. an increase in the salt content of the corrodent enhances the impingement attack;

5. a decrease in the oxygen content of the corrodent reduces the degree of impingement attack.

The two major conclusions which can be drawn from the results of this investigation are the following:

1. unalloyed titanium, in view of the absence of corrosion and stress corrosion, is an excellent candidate material for desalination service; recent cost reductions should increase its attraction;

2. although service history has shown that Cu-Ni alloys perform satisfactorily in desalination service, care must be exercised to effect the necessary feedwater deaeration in order to reduce otherwise high corrosion rates in sea-salt solutions to acceptable levels. end

end

8. ACKNOWLEDGMENTS

The invaluable technical assistance of H. M. Warren is gratefully acknowledged. The author is also indebted to the Anaconda American Brass Company for the provision of the copper-nickel sheet, and to the Scovill Manufacturing Company for supplying the 70Cu-30Ni tubing. Special thanks are due to S. F. Mulford at the OSW Saline Water Test Facility in San Diego for the provision of the seawater and 7% sea-salt brine, and to W. C. Stamper at the OSW Demonstration Plant in Roswell, N. M., for the brackish well water.

9. REFERENCES

1. H. I. Logan, The Stress Corrosion of Metals, John Wiley and Sons, N. Y., p. 156 (1966).

2. H. H. Uhlig, Corrosion and Corrosion Control, John Wiley and Sons, N. Y., p. 294 (1963).

3. D. H. Thompson and A. W. Tracy, Trans. AIME 185, 100 (1949).

4. ASM Metals Handbook, 8th Ed. 1, 1000 (1961).

5. F. L. LaQue and H. R. Copson, Corrosion Resistance of Metals and Alloys, 2nd Ed., Reinhold Publishing Corp., N. Y., p. 579 (1963).

6. E. H. Newton and J. D. Birkett, "Survey of Materials Behavior in Multi-Stage Flash Distillation Plants," Summary Report, Arthur D. Little, Inc., Sept. 25 (1968).

7. A. H. Tuthill and D. A. Sudrabin, Metals Eng. Quarterly 7, No. 3, 10 (1967).

8. B. F. Brown and C. D. Beachem, Corr. Sci. 5, 745 (1965).

9. B. F. Brown, Mat. Res. and Standards 6, March (1966).

10. B. F. Brown, et al., "Marine Corrosion Studies," NRL Memo Rep. 1634, July (1965).

11. I. R. Lane, J. L. Cavallero, and A. G. S. Morton, Stress Corrosion Cracking of Titanium, ASTM STP 397, 246 (1966).

12. A. J. Hatch, H. W. Rosenberg, and E. F. Erlien, p. 122, Ref. 11.

13. G. Sanderson and J. C. Scully, Nature 211, 179 (1966).

14. E. O. Hall, Proc. Phys. Soc. (London) B64, 747 (1951).

15. N. J. Petch, J. Iron Steel Inst. 174, 25 (1953).

16. R. W. Armstrong, I. Codd, R. M. Douthwaite, and N. J. Petch, Phil. Mag. 7, 45 (1962).

17. R. N. Orava, "The Effect of Grain Size on the Yielding and Flow of Molybdenum," Physical Metallurgy of the Refractory Metals, ed. R. I. Jaffee and J. Maltz, Gordon and Breach, in press.

18. R. N. Orava, G. Stone, and H. Conrad, Trans. ASM 59, 171 (1966).

19. W. C. Stewart and F. L. LaQue, Corrosion 8, 259 (1952).

20. ASM Metals Handbook, 8th Ed. 1, 1030 (1961).

21. International Nickel Co., Basic Engineering Data on Copper-Nickel Alloys.

22. Titanium Design Data Handbook, Titanium Metals Corporation of America.

23. G. Haaijer and A. W. Loginow, Corrosion 21, 105 (1965).

24. G-1 Committee on Corrosion of Metals, "Stress Corrosion Testing Methods," Stress Corrosion Testing, ASTM STP 425, p. 3 (1967).

25. F. H. Haynie and W. K. Boyd, "Stress Corrosion Cracking of Aluminum Alloys," DMIC Report 228, July 1 (1966).

26. N. G. Feige and R. L. Kane, Metals Eng. Quarterly 7, No. 3, 27 (1967).

27. ASM Metals Handbook, 8th Ed. 1, 985 (1961).

28. P. T. Gilbert, Corrosion, ed. L. L. Schreir, John Wiley and Sons, N. Y., p. 4.49 (1963).

29. N. D. Tomashov, Theory of Corrosion and Protection of Metals, MacMillan Co., N. Y. (1966).